

**SECOND EUROPEAN SUMMER SCHOOL on  
MICROSCOPIC QUANTUM MANY-BODY THEORIES  
and their APPLICATIONS**

**(3 - 14 September 2001)**

---

**ELEMENTARY EXCITATIONS AND  
DYNAMIC STRUCTURE OF QUANTUM FLUIDS  
Part II**

**Mikko SAARELA  
University of Oulu  
Department of Physical Sciences/Theoretical Physics  
P.O. Box 3000  
Oulu, FIN-90014  
FINLAND  
ITALY**

---

These are preliminary lecture notes, intended only for distribution to participants



# Elementary excitations and dynamic structure of quantum fluids

Doc. M. Saarela,

Department of Physical Sciences/Theoretical Physics,  
University of Oulu,  
PL3000,  
FIN-90401,  
Finland

14th September 2001

**Material for reading:**

**Jesús Navarro and Artur Polls (Eds.):**

*Microscopic Quantum Many-Body Theories and Their Applications* ,

**Lecture Notes in Physics, Springer-Verlag, Berlin, 1998**

# Contents

<b>1</b>	<b>Introduction: historical developments</b>	<b>2</b>
<b>2</b>	<b>Optimized ground state</b>	<b>4</b>
2.1	Feenberg's prime-derivative technique . . . . .	5
<b>3</b>	<b>Equation of motion method</b>	<b>7</b>
3.1	Linear response theory . . . . .	8
3.2	Time-dependent correlation functions . . . . .	9
3.3	Action integral . . . . .	10
3.4	Least action principle . . . . .	11
3.5	Many-particle densities . . . . .	12
3.6	Many-particle currents . . . . .	13
3.7	Continuity equations in homogeneous fluids . . . . .	13
<b>4</b>	<b>Solving the continuity equations</b>	<b>14</b>
4.1	Feynman approximation . . . . .	15
<b>5</b>	<b>CBF-approximation</b>	<b>17</b>
5.1	Convolution approximation . . . . .	17
5.2	Two-particle equation . . . . .	18
5.3	One-particle equation . . . . .	21
5.4	Self-energy . . . . .	22
5.5	Numerical solution . . . . .	23
5.6	Analytic structure of the self-energy . . . . .	24
5.7	Anomalous dispersion in liquid $^4\text{He}$ . . . . .	25
5.8	Absolute minimum in the spectrum . . . . .	30
<b>6</b>	<b>The full solution</b>	<b>31</b>
6.1	Continuity equations . . . . .	32
6.2	Continuity equations in momentum space . . . . .	34
6.3	Phonon-roton spectrum . . . . .	39
6.4	Results on two-particle currents . . . . .	39
6.5	Precursor of the liquid-solid transition . . . . .	41
6.6	Results in liquid $^4\text{He}$ . . . . .	41
6.7	Results in charged Yukawa Bose gas . . . . .	42
<b>7</b>	<b>Sum rules</b>	<b>49</b>
<b>8</b>	<b>Dynamics of a single impurity</b>	<b>53</b>
8.1	Continuity equations . . . . .	53
8.2	Linear response and self energy . . . . .	54
8.3	Hydrodynamic effective mass . . . . .	56
8.4	Results . . . . .	56
<b>9</b>	<b>Summary</b>	<b>61</b>

# 1 Introduction: historical developments

Compared to the ground state, the basic theoretical understanding of the microscopic structure of the excitations and of the physical processes involved is relatively incomplete. On the experimental side, however, the elementary excitation spectrum of liquid  ${}^4\text{He}$ , along with the underlying dynamic structure function, are known to a **high precision from x-ray and neutron scattering experiments**. (A review of the subject with references to earlier experimental and theoretical work is given by Glyde in his book.[1]) Thus, modern many-body methods face a demanding challenge of reproducing the correct spectrum; a solid agreement would create confidence in the applied tools and indicate that the essential physical ingredients have been understood and included into the calculations. A fully microscopic approach is needed here, because these phenomena defy a simple hydrodynamic Al description.

Before bringing the variational point of view into play, let us quickly summarize the milestones on this path. The preliminary work on the subject was done by Bijl and Landau in the 1940s.[2] **Landau** proposed that there are two separate collective excitation modes in liquid  ${}^4\text{He}$ : **phonons**, thought of as collective density (sound) modes having linear dispersion, and **rotons**, assumed to be a collective rotation of the fluid having a separate dispersion curve. Later on, he joined these excitations into a single collective mode dispersion curve continuous in the wave vector. Phonons and rotons were then interpreted as the low- and high- $k$  regions of the same collective excitation. (In this sense the name “roton” is a misnomer.) Between them we have what is called the **maxon** region. This seemed to be in qualitative agreement with experimental data and, at the same time, consistent with the continuous dispersion curve for excitations in a dilute Bose gas derived microscopically by Bogoliubov in his seminal paper.[3]

After these early developments **Feynman** took the first steps towards a microscopic description by suggesting a specific trial excited-state wave function.[4] Specifically, he wrote the wave function of the excited state  $\Psi_{\mathbf{k}}$  of momentum  $\hbar\mathbf{k}$  as a product  $\Psi_{\mathbf{k}} = \rho_{\mathbf{k}}\Psi_0$  of the ground-state wave function  $\Psi_0$  and of a density-fluctuation operator  $\rho_{\mathbf{k}} = \sum_j \exp(i\mathbf{k}\cdot\mathbf{r}_j)$ , offering thus a microscopic explanation for phonons and rotons as collective density excitations at all  $k$ . Although the spectrum calculated variationally using the proposed wave function, leading to the dispersion relation

$$\varepsilon_F(k) = \frac{\hbar^2 k^2}{2mS(k)} \quad (1)$$

seemed to contain much of the relevant physics, quantitatively the agreement was far from being satisfactory. The dispersion relation (1) does provide an upper bound for the lowest-lying excitation and is exact in the long-wavelength limit, but has severe deficiencies at shorter wavelengths.

For example, the computed roton energy is twice as large as the experimentally observed value. Owing to this discrepancy, the theory was subsequently supplemented by Feynman and Cohen[5] to include so-called **backflow corrections**

which increased the flexibility of the wave function and, thus, lowered the roton energy significantly towards measured values. The term backflow is used to describe the correlated motion of neighboring particles around a given reference atom. In the initial picture put forward by Feynman and Cohen the form of this backflow was not unconstrained: instead, they assumed that the particles move in a dipolar flow field, behaving in a sense like a smoke ring.

After Feynman's original arguments the method of correlated basis functions (CBF) was developed along the same lines to further improve the agreement between theoretical predictions and experimental data, most notably by **Feenberg** and his collaborators,[6, 7, 8, 9, 10] In the **CBF approach** the excited-state wave function  $\Psi_{\mathbf{k}}$  is written as  $\Psi_{\mathbf{k}} = F_{\mathbf{k}}\Psi_0$ , and the excitation operator  $F_{\mathbf{k}}$  is further expressed as a **polynomial in the density-fluctuation operators**  $\{\rho_{\mathbf{k}}\}$ . Thus, in the lowest order we have the usual Feynman form for the excited states, and terms beyond the linear one introduce the backflow effects. Attempts to calculate the dynamic structure function were also made.[11]

More recently the **shadow wave function (SWF) method** has been extended to permit the investigations of excited states.[12, 13] By the provision that the momentum-carrying factor in  $\Psi_{\mathbf{k}}$  is a density fluctuation in the subsidiary (shadow) variables, one has, in principle, a parameter-free wave function of the Feynman form in which the fluctuations in the subsidiary variables allow for the presence of backflow effects in the particle variables. Again, this backflow is represented by terms of all orders in the density fluctuation  $\{\rho_{\mathbf{k}}\}$  of the real variables. The CBF and SWF methods, along with the application of **released-node Monte Carlo simulations**, all give results which agree reasonably well with experimental data.

Three-dimensional **vortex rings** are also candidates for rotons, and expanding rings could account for the lambda transition.[14] One additional view to the problem is that unlike phonons, rotons might involve the motion of only few  $^4\text{He}$  atoms, a group forming a **quasi-particle**. In the extreme case this quasi-particle would be just one atom dressed in a superfluid backflow.[15] In the novel picture put forward by Glyde and Griffin the roton is viewed as a **renormalized single-particle mode**. This model has been used extensively to analyze neutron scattering data.[16, 1, 17]

The excitation spectrum of liquid  $^4\text{He}$  is in two dimensions qualitatively very similar to the three-dimensional spectrum, as one might expect since the physics of liquid  $^4\text{He}$  is dominated by short-range correlations. What makes the 2D system especially interesting, however, is that the **vortex-antivortex pair excitation** occurs there naturally as a low-lying elementary excitation mode. [18, 19, 20, 21, 22, 23] Therefore, this system forms an ideal framework within which it is possible to study the specific differences between the roton and vortex excitations.

**The equation motion method** for excited states and dynamics of quantum fluids and fluid mixtures which I will present here has its roots in the early works by Saarela and Suominen.[24, 25, 26] and by Krotscheck[27]. In that method

one starts with an Hamiltonian which contains an infinitesimal, external, dynamic interaction which drives excitations into the system and then one looks for the response in the one- and two-particle density distributions. The time dependence of the external interaction creates currents into the system, which are solved together with the density fluctuations from the equations of motion. We limit ourselves into the linear response and thus calculate the **linear response function** and from that the **dynamic structure function**. The method has been applied to homogeneous and inhomogeneous quantum fluids and their mixtures.

To **summarize** our present understanding of the dynamic structure of liquid  ${}^4\text{He}$ .

The nature of the collective excitations is fairly well understood.

The role of the Bose condensate in the excitations needs to be clarified.

Quantitative understanding of the behavior of the dynamic structure function  $S(k, \omega)$  is still missing.

## 2 Optimized ground state

In the **microscopic variational theory** we start from the empirical Hamiltonian for the system of  $N$  particles with mass  $m$

$$H_0 = - \sum_{i=1}^N \frac{\hbar^2}{2m} \nabla_i^2 + \frac{1}{2} \sum_{i \neq j}^N V(|\mathbf{r}_i - \mathbf{r}_j|). \quad (2)$$

We assume that the two-particle interaction  $V(|\mathbf{r}_i - \mathbf{r}_j|)$  is known.

For the **variational wave function** we take the Jastrow-Feenberg ansatz [6, 28, 7]

$$\begin{aligned} \Psi_0(\mathbf{r}_1, \dots, \mathbf{r}_N) &= e^{\frac{1}{2}U(\mathbf{r}_1, \dots, \mathbf{r}_N)} \Phi_0(\mathbf{r}_1, \dots, \mathbf{r}_N) \\ U(\mathbf{r}_1, \dots, \mathbf{r}_N) &= \frac{1}{2} \sum_{i \neq j}^N u_2(\mathbf{r}_i, \mathbf{r}_j) \\ &\quad + \frac{1}{3!} \sum_{i \neq j \neq k}^N u_3(\mathbf{r}_i, \mathbf{r}_j, \mathbf{r}_k) \end{aligned} \quad (3)$$

The **variational problem** is to minimize the total energy

$$E_0 = \frac{\langle \Psi_0 | H_0 | \Psi_0 \rangle}{\langle \Psi_0 | \Psi_0 \rangle} \quad (4)$$

with respect to the correlation functions  $u_2(\mathbf{r}_i, \mathbf{r}_j)$  and  $u_3(\mathbf{r}_i, \mathbf{r}_j, \mathbf{r}_k)$ . This leads to the Euler equations

$$\frac{\delta E_0}{\delta u_2(\mathbf{r}_1, \mathbf{r}_2)} = 0 \quad (5)$$

$$\frac{\delta E_0}{\delta u_3(\mathbf{r}_1, \mathbf{r}_2, \mathbf{r}_3)} = 0 \quad (6)$$

## 2.1 Feenberg's prime-derivative technique

Let's derive the Euler equation by using Feenberg's prime-derivative technique [6]. By definition we have

$$u_2(r; \lambda) \equiv u_2(r) + \lambda \left[ V(r) - \frac{\hbar^2}{4m} \nabla^2 u_2(r) \right] \quad (7)$$

where  $V(r)$  is the two-particle interaction. In the following we use the notation

$$u_2'(r) = \left. \frac{\partial u_2(r; \lambda)}{\partial \lambda} \right|_{\lambda=0} \quad (8)$$

and ignore  $\lambda$  from the list of arguments of the functions. Then

$$u_2'(r) = V(r) - \frac{\hbar^2}{4m} \nabla^2 u_2(r) \quad (9)$$

**Arturo Polls** showed to you how to write the energy/particle in the form

$$\frac{E}{N} = \frac{1}{2} \rho_0 \int d^3r g(r) \left[ V(r) - \frac{\hbar^2}{2m} \nabla^2 u_2(r) \right] \quad (10)$$

where  $g(r)$  is the **radial distribution function** and the derived the Euler equation (5) both in coordinate space

$$g'(r) = \frac{\hbar^2}{4m} \nabla^2 g(r) \quad (11)$$

and in momentum space

$$S'(k) = -\frac{\hbar^2 k^2}{4m} (S(k) - 1) \quad (12)$$

using the structure function  $S(k)$ .

$$S(k) = 1 + \rho_0 \int d^3r (g(r) - 1) e^{i\mathbf{k}\cdot\mathbf{r}} \quad (13)$$

Let us define two new quantities the **induced potential** in terms of the sum of nodal diagrams  $N(r)$  as

$$w_{\text{ind}}(r) = N'(r) + \frac{\hbar^2}{4m} \nabla^2 N(r), \quad (14)$$



and the **particle-hole effective interaction** in terms of the direct correlation function  $X(r)$

$$V_{p-h}(r) = X'(r) + \frac{\hbar^2}{4m} \nabla^2 X(r) \quad (15)$$

The **HNC-equation** connects these quantities

$$g(r) = e^{u_2(r)+N(r)} \quad (16)$$

$$\Rightarrow u_2(r) = \log g(r) - N(r) \quad (17)$$

$$g'(r) = g(r) (u_2'(r) + N'(r)) \quad (18)$$

Inserting  $u_2(r)$  into the definitions (9) and (18) we get

$$\begin{aligned} g'(r) &= g(r)V(r) + g(r)N'(r) \\ &+ \frac{\hbar^2}{4m} \left[ 4 \left( \nabla \sqrt{g(r)} \right)^2 - \nabla^2 g(r) + g(r) \nabla^2 N(r) \right] \end{aligned} \quad (19)$$

Subtract  $N'(r)$  from both sides of Eq. (19) and use the **definitions**

$$\begin{aligned} X(r) &= g(r) - 1 - N(r) \\ X'(r) &= g'(r) - N'(r). \end{aligned} \quad (20)$$

Then

$$\begin{aligned} X'(r) &= g(r)V(r) \\ &+ (g(r) - 1) \left[ N'(r) + \frac{\hbar^2}{4m} \nabla^2 N(r) \right] \\ &+ \frac{\hbar^2}{4m} \left[ 4 \left( \nabla \sqrt{g(r)} \right)^2 - \nabla^2 X(r) \right] \end{aligned} \quad (21)$$

Inserting the definitions (14) and (15) we get the expression for the particle-hole potential

$$\begin{aligned} V_{p-h}(r) &= g(r)V(r) + (g(r) - 1) w_{\text{ind}}(r) \\ &+ \frac{\hbar^2}{m} \left( \nabla \sqrt{g(r)} \right)^2 \end{aligned} \quad (22)$$

On the other hand from the **Ornstein-Zernike relation**

$$N(|\mathbf{r}_1 - \mathbf{r}_2|) = \int d^3 r_3 (g(|\mathbf{r}_1 - \mathbf{r}_3|) - 1) X(|\mathbf{r}_3 - \mathbf{r}_2|) \quad (23)$$

together with the definition (20) we get

$$\tilde{X}(k) = 1 - \frac{1}{S(k)} \quad (24)$$

The priming operation and the use of Eq. (12) gives

$$\tilde{X}'(k) = \frac{S'(k)}{S^2(k)} = -\frac{\hbar^2 k^2 (S(k) - 1)}{4m S^2(k)} \quad (25)$$

Inserting these into the definition (15) we get

$$\begin{aligned} \tilde{V}_{p-h}(k) &= -\frac{\hbar^2 k^2}{4m} \left( \frac{S(k) - 1}{S^2(k)} + \frac{S(k) - 1}{S(k)} \right) \\ &= -\frac{\hbar^2 k^2}{4m} \left( 1 - \frac{1}{S^2(k)} \right) \end{aligned} \quad (26)$$

which is the **Euler equation** for the homogeneous one-component quantum fluid,

$$S(k) = \frac{k}{\sqrt{k^2 + \frac{4m}{\hbar^2} \tilde{V}_{p-h}(k)}} \quad (27)$$

We still need to calculate the **induced potential**  $w_{ind}(r)$  defined in Eq. (14). From the Ornstein-Zernike we get

$$\tilde{N}(k) = \frac{(S(k) - 1)^2}{S(k)} \quad (28)$$

The priming operation and the use of Eqs. (12) and (25) gives

$$\tilde{N}'(k) = S'(k) - \tilde{X}'(k) = -\frac{\hbar^2 k^2 (S(k) - 1)^2 (S(k) + 1)}{4m S^2(k)} \quad (29)$$

Inserting these into the definition (14) we get

$$\begin{aligned} \tilde{w}_{ind}(k) &= -\frac{\hbar^2 k^2}{4m} (S(k) - 1)^2 \left( \frac{S(k) + 1}{S^2(k)} + \frac{1}{S(k)} \right) \\ &= -\frac{\hbar^2 k^2}{4m} (2S(k) + 1) \left( 1 - \frac{1}{S(k)} \right)^2 \end{aligned} \quad (30)$$

### 3 Equation of motion method

We begin with an assumption that the correlation functions in the ground state wave function are optimized. It means that the system is stable against small perturbations (linear) around that solution. Let us assume that we disturb the system with an infinitesimal, external interaction. The system responds to that by changing its density, but because it is in the optimized ground state all terms linear in small changes in correlation functions disappear.

$$\frac{E}{N} = \frac{E_0}{N} + \frac{\delta E/N}{\delta U} \Big|_{\min} \delta U + \frac{1}{2} \frac{\delta^2 E/N}{\delta U^2} \Big|_{\min} [\delta U]^2 + O[\delta U^3] \quad (31)$$

and one is left with the quadratic terms. Using the least action principle we can derive the continuity equations which optimize the fluctuations in the correlation functions and give the change in the density caused by the infinitesimal external disturbance. These ideas lead to the linear response theory.

### 3.1 Linear response theory

Let us disturb the system using an external interaction  $U_{\text{ext}}(k, \omega)$  with a given frequency  $\omega$  and wave number  $k$ . The change in the density of a homogeneous system  $\delta\rho_1(k, \omega)$  will have the same frequency and wave number and the information of the dynamic properties of the system is contained in the **linear-response function** defined as

$$\chi(k, \omega) = \frac{\delta\tilde{\rho}_1(\mathbf{k}; \omega)}{\rho_0 U_{\text{ext}}(k, \omega)}, \quad (32)$$

The imaginary part of the linear-response function defines the **dynamic structure function**

$$S(k, \omega) = -\frac{1}{2\pi} \Im m [\chi(k, \omega)], \quad (33)$$

which is the measured quantity in the scattering experiments.

At low temperatures  $S(k, \omega)$  consists of a sharp peak and of a broad contribution. It is therefore customary to write  $S(k, \omega)$  as

$$S(k, \omega) = Z(k)\delta(\omega - \omega_0(k)) + S_{\text{mp}}(k, \omega). \quad (34)$$

This suggests that the linear response function can be written in the form

$$\chi(k, \omega) = \frac{2S(k)}{\hbar\omega - \hbar\omega' - \Sigma(k, \omega')} \quad (35)$$

The quantity  $Z(k)$ , the residue of the response function at the pole  $\omega = \omega_0(k)$ , can be evaluated from the derivative of the **self energy**  $\Sigma(k, \omega)$

$$Z(k) = \left[ 1 - \left. \frac{d\Sigma(k, \omega)}{d(\hbar\omega)} \right|_{\omega=\omega_0} \right]^{-1}, \quad (36)$$

and gives the strength of the sharp peak, whereas  $S_{\text{mp}}(k, \omega)$  gives what is called the **multi-phonon background**, *i.e.* the contribution in which the neutron probing the system exchanges energy with two or more excitations.

In addition, the relative weight  $Z(k)/S(k)$  gives the efficiency of the single collective excitation scattering processes, as seen from the (zeroth-moment) **sum rule**

$$\int_0^\infty S(k, \omega) d\omega = S(k) = \langle \rho_{-\mathbf{k}} \rho_{\mathbf{k}} \rangle / N \quad (37)$$

In other words it gives the fraction of the available scattering processes at a given wave number, which go through a single collective mode. If the excitation were a simple density wave, as assumed in the **Feynman theory**, this ratio would be

$$\frac{Z(k)}{S(k)} = 1 \quad (38)$$

### 3.2 Time-dependent correlation functions

If a weak, time dependent interaction perturbs the system then the ground-state wave function,  $\Psi_0(\mathbf{r}_1, \dots, \mathbf{r}_N)$ , is modified accordingly and the correlation functions become time dependent,

$$\Psi(\mathbf{r}_1, \dots, \mathbf{r}_N; t) = e^{-iE_0 t/\hbar} \Phi(\mathbf{r}_1, \dots, \mathbf{r}_N; t) \quad (39)$$

with

$$\begin{aligned} \Phi(\mathbf{r}_1, \dots, \mathbf{r}_N; t) &= \frac{1}{\sqrt{\mathcal{N}(t)}} \phi(\mathbf{r}_1, \dots, \mathbf{r}_N; t) \\ \phi(\mathbf{r}_1, \dots, \mathbf{r}_N; t) &= e^{\frac{1}{2}\delta U(\mathbf{r}_1, \dots, \mathbf{r}_N; t)} \Psi_0(\mathbf{r}_1, \dots, \mathbf{r}_N). \end{aligned} \quad (40)$$

The **excitation operator**

$$\delta U(\mathbf{r}_1, \dots, \mathbf{r}_N; t) = \sum_i \delta u_1(\mathbf{r}_i; t) + \sum_{i < j} \delta u_2(\mathbf{r}_i, \mathbf{r}_j; t) \quad (41)$$

is a complex function and represents fluctuations in the correlation functions due to this external perturbation.

The time-dependent **one-body function**  $\delta u_1(\mathbf{r}_i; t)$  must be included into the description since the dynamics will normally break the translational invariance of the system, but restricting the time dependence to the one-body component only would lead directly to the Feynman theory of excitations.

The time-dependent **two-body component** is significant in situations where the external field excites fluctuations of wavelengths comparable to the inter-particle distance, as explicitly demonstrated in Refs. [29, 25, 26, 24, 10] for liquid  $^4\text{He}$  and in Ref. [30] for the bosonic Coulomb system. With these terms included the excitation operator then has a two-phonon basis,

$$\sum_{i,j} \delta u_2(\mathbf{r}_i, \mathbf{r}_j; t) = \int \frac{d^3 k_1 d^3 k_2}{(2\pi)^6 \rho_0} \delta u_2(\mathbf{k}_1, \mathbf{k}_2; t) \rho_{\mathbf{k}_1} \rho_{\mathbf{k}_2}. \quad (42)$$

In the wave function (40) the **optimized** ground state  $\Psi_0(\mathbf{r}_1, \dots, \mathbf{r}_N)$  satisfies the Schrödinger equation

$$H_0 \Psi_0 = E_0 \Psi_0 \quad (43)$$

where  $H_0$  is the **ground state Hamiltonian** given in Eq. (2) and  $E_0$  appearing in the phase factor of definition Eq. (39) is the **ground state energy**. The

**normalization factor** contains the ratio between the ground state and excited state normalizations.

$$\mathcal{N}(t) = \frac{\int d^3r_1 \dots d^3r_N |\Psi_0(\mathbf{r}_1, \dots, \mathbf{r}_N)|^2 e^{\Re e[\delta U(\mathbf{r}_1, \dots, \mathbf{r}_N; t)]}}{\langle \Psi_0 | \Psi_0 \rangle} \quad (44)$$

### 3.3 Action integral

**The new Hamiltonian**

$$H(t) = H_0 + \sum_i U_{\text{ext}}(\mathbf{r}_i; t). \quad (45)$$

which contains the infinitesimal external potential  $U_{\text{ext}}(\mathbf{r}; t)$  is now time dependent and must satisfy the least-action principle [31, 32]

$$\begin{aligned} \delta S &= \delta \int_{t_0}^t dt' \mathcal{L}(t') \\ &= \delta \int_{t_0}^t dt' \left\langle \Psi(t') \left| H(t) - i\hbar \frac{\partial}{\partial t'} \right| \Psi(t') \right\rangle = 0, \end{aligned} \quad (46)$$

We make two **assumptions** in the evaluation of the action integral. Firstly, we require that the ground-state correlation functions are **optimized**. This is important because it eliminates all contributions to the action integral that are linear in the time-dependent correlation functions. Secondly, we assume that the **perturbation is weak** which allows us to keep only the quadratic terms – and warrants the use of the **linear-response theory**.

Using the ground state Schrödinger equation (43) we can write the **integrand** in the form

$$\begin{aligned} \mathcal{L}(t) &= \left\langle \Phi(t) \left| H - E_0 - \frac{\hbar}{2} \left( i \frac{\partial}{\partial t} + h.c. \right) \right| \Phi(t) \right\rangle \\ &= \frac{1}{\mathcal{N}(t)} \left\langle \Psi_0 \left| e^{\frac{1}{2}\delta U^*(t)} [H_0, e^{\frac{1}{2}\delta U(t)}] \Psi_0 \right\rangle \\ &+ \left\langle \Phi \left| -\frac{\hbar}{2} \left( i \frac{\partial}{\partial t} + h.c. \right) + U_{\text{ext}}(t) \right| \Phi \right\rangle \end{aligned} \quad (47)$$

The potential energy term commutes with  $\delta U(t)$  and thus only the **kinetic energy** gives contribution to the commutator. This can be evaluated with a little bit of algebra,

$$\begin{aligned} &\int d\tau \Psi_0 e^{\frac{1}{2}\delta U^*} \nabla^2 \left( e^{\frac{1}{2}\delta U} \Psi_0 \right) \\ &= \int d\tau \Psi_0 e^{\frac{1}{2}\delta U^*} \nabla \cdot \left( \frac{1}{2} e^{\frac{1}{2}\delta U} \Psi_0 \nabla \delta U + e^{\frac{1}{2}\delta U} \nabla \Psi_0 \right) \end{aligned}$$

$$\begin{aligned}
&= \int d\tau \left[ -e^{\frac{1}{2}\delta U^*} \left( \frac{1}{2}\Psi_0 \nabla \delta U^* + \nabla \Psi_0 \right) \frac{1}{2} e^{\frac{1}{2}\delta U} \Psi_0 \nabla \delta U \right. \\
&+ \left. \Psi_0 e^{\Re[\delta U]} \left( \frac{1}{2} \nabla \Psi_0 \cdot \nabla \delta U + \nabla^2 \Psi_0 \right) \right] \\
&= \int d\tau \left[ -\frac{1}{4} |\Psi_0|^2 e^{\Re[\delta U]} |\nabla \delta U|^2 + \Psi_0 e^{\Re[\delta U]} \nabla^2 \Psi_0 \right],
\end{aligned}$$

giving the result

$$\begin{aligned}
&\frac{1}{\mathcal{N}(t)} \left\langle \Psi_0 \left| e^{\frac{1}{2}\delta U^*} [H_0, e^{\frac{1}{2}\delta U}] \right| \Psi_0 \right\rangle \\
&= \frac{\hbar^2}{8m} \left\langle \Phi \left| \sum_{j=1}^N |\nabla_j \delta U|^2 \right| \Phi \right\rangle
\end{aligned} \tag{48}$$

The evaluation of the **time derivative** gives

$$\begin{aligned}
&-\frac{\hbar}{2} \left\langle \Psi_0 \left| \frac{e^{\frac{1}{2}\delta U^*(t)}}{\sqrt{\mathcal{N}(t)}} \left( i \frac{\partial}{\partial t} + h.c. \right) \frac{e^{\frac{1}{2}\delta U(t)}}{\sqrt{\mathcal{N}(t)}} \right| \Psi_0 \right\rangle \\
&= \frac{1}{2} \hbar \left\langle \Phi \left| \Im m[\delta \dot{U}(t)] \right| \Phi \right\rangle
\end{aligned} \tag{49}$$

where we have used the dot-notation  $\dot{f}(t) = \frac{\partial f(t)}{\partial t}$ .

Collecting all together we have the integrand

$$\mathcal{L}(t) = \left\langle \Phi \left| \frac{\hbar^2}{8m} \sum_{j=1}^N |\nabla_j \delta U|^2 + \frac{1}{2} \hbar \Im m[\delta \dot{U}] + U_{ext} \right| \Phi \right\rangle \tag{50}$$

### 3.4 Least action principle

In the **least action principle** we search for the correlation function which minimizes the action integral (46). Let's assume that our excitation operator  $\delta U = \delta U(\mathbf{r}_1, \dots, \mathbf{r}_n; t)$  depends on  $n$  coordinates and the time. Then the variation of the action integral

$$\delta \mathcal{S} = \delta \int_{t_0}^t dt' \mathcal{L}(t') = 0 \tag{51}$$

with respect to  $\delta U^*$  gives

$$\begin{aligned}
&\int dr_{n+1} \dots dr_N \left[ -\frac{\hbar^2}{8m} \sum_{j=1}^n \nabla_j \cdot (|\Phi|^2 \nabla_j \delta U) \right. \\
&- \left. \frac{i\hbar}{4} \frac{\partial}{\partial t} |\Phi|^2 + \left( \frac{\hbar}{2} \Im m[\delta \dot{U}] + U_{ext} \right) \frac{1}{\mathcal{N}(t)} \frac{\partial |\phi|^2}{\partial \delta U^*} \right] \\
&- \left\langle \Phi \left| \frac{\hbar}{2} \Im m[\delta \dot{U}] + U_{ext} \right| \Phi \right\rangle \frac{1}{\mathcal{N}(t)} \frac{\partial \mathcal{N}(t)}{\partial \delta U^*}
\end{aligned} \tag{52}$$

The derivatives can be calculated from the definitions (40)

$$\begin{aligned}\frac{\partial|\phi|^2}{\partial\delta U^*} &= \frac{1}{2}|\phi|^2 \\ \frac{1}{\mathcal{N}}\frac{\partial\mathcal{N}}{\partial\delta U^*} &= \frac{1}{2}\int dr_{n+1}\dots dr_N|\Phi|^2 \\ \frac{\partial}{\partial t}|\Phi|^2 &= |\Phi|^2\left[\Re e\delta\dot{U} - \int dr_1\dots dr_N|\Phi|^2\Re e\delta\dot{U}\right]\end{aligned}$$

and the **least action principle** can be written in the form

$$\begin{aligned}\int dr_{n+1}\dots dr_N\left[-\frac{\hbar^2}{4m}\sum_{j=1}^n\nabla_j\cdot(|\Psi|^2\nabla_j\delta U)\right. \\ \left.+|\Psi|^2\left(-\frac{i\hbar}{2}\delta\dot{U} + U_{ext}\right)\right. \\ \left.-|\Psi|^2\left\langle\Psi\left|-\frac{i\hbar}{2}\delta\dot{U} + U_{ext}\right|\Psi\right\rangle\right] = 0\end{aligned}\quad (53)$$

### 3.5 Many-particle densities

In order to simplify Eq. (53) we define the *n*-particle density,

$$\begin{aligned}\rho_n(\mathbf{r}_1,\dots,\mathbf{r}_n;t) \\ = \frac{N!}{(N-n)!}\int d^3r_{n+1}\dots d^3r_N|\Psi(\mathbf{r}_1,\dots,\mathbf{r}_N;t)|^2\end{aligned}\quad (54)$$

In the linear response theory one assumes that the time dependent perturbation of the system is infinitesimal and hence we can separate the time dependent and independent parts in the density,

$$\rho_n(\mathbf{r}_1,\dots,\mathbf{r}_n;t) = \bar{\rho}_n(\mathbf{r}_1,\dots,\mathbf{r}_n) + \delta\rho_n(\mathbf{r}_1,\dots,\mathbf{r}_n;t)\quad (55)$$

Expanding to the first order in  $\delta U$  we get

$$\begin{aligned}\delta\rho_n(\mathbf{r}_1,\dots,\mathbf{r}_n;t) &= \frac{N!}{(N-n)!}\int dr_{n+1}\dots dr_N|\Psi_0|^2 \\ &\times \left[\delta U - \langle\Psi_0|\delta U|\Psi_0\rangle\right]\end{aligned}\quad (56)$$

The physical density is a real quantity and  $\delta U$  should be replaced with its real part. Here we have generalized the definition to complex density fluctuations.

### 3.6 Many-particle currents

Similarly we define the  $n$ -particle current

$$\begin{aligned} & \mathbf{j}_n(\mathbf{r}_1, \dots, \mathbf{r}_n; t) & (57) \\ &= \frac{\hbar}{2mi} \frac{N!}{(N-n)!} \int d^3r_{n+1} \dots d^3r_N \end{aligned}$$

$$\begin{aligned} & \Psi^*(\mathbf{r}_1, \dots, \mathbf{r}_N; t) \sum_{j=1}^n \nabla_j \Psi(\mathbf{r}_1, \dots, \mathbf{r}_N; t) \\ & \approx \frac{\hbar}{2mi} \frac{N!}{(N-n)!} \int d^3r_{n+1} \dots d^3r_N \\ & |\Psi_0(\mathbf{r}_1, \dots, \mathbf{r}_N)|^2 \sum_{j=1}^n \nabla_j \delta U & (58) \end{aligned}$$

### 3.7 Continuity equations in homogeneous fluids

Let us assume that our system is homogeneous and the single-particle density of the ground state is constant.

$$\bar{\rho}_1(\mathbf{r}) = \rho_0 = \text{constant} \quad (59)$$

It is convenient to introduce the  $n$ -particle distribution function

$$g_n(\mathbf{r}_1, \dots, \mathbf{r}_n) = \frac{1}{(\rho_0)^n} \bar{\rho}_n(\mathbf{r}_1, \dots, \mathbf{r}_n) \quad (60)$$

With these assumptions we derive the **one- and two-particle continuity equations** from the general Euler equation (53). These are the **equations of motion** of the system [29, 25, 26]

$$\nabla_1 \cdot \mathbf{j}_1(\mathbf{r}_1; t) + i\delta\dot{\rho}_1(\mathbf{r}_1; t) = D_1(\mathbf{r}_1; t) \quad (61)$$

$$\begin{aligned} & [\nabla_1 \cdot \mathbf{j}_2(\mathbf{r}_1, \mathbf{r}_2; t) + \text{same for } (1 \leftrightarrow 2)] \\ & + i\delta\dot{\rho}_2(\mathbf{r}_1, \mathbf{r}_2; t) = D_2(\mathbf{r}_1, \mathbf{r}_2; t). \end{aligned} \quad (62)$$

The **terms with time derivatives** in Eq. (53) are exactly time derivatives of the density. Inserting the definition of the excitation operator (41) into the definition of the density (56) we get for the one-particle density

$$\begin{aligned} & \delta\rho_1(\mathbf{r}_1; t) = \rho_0 \delta u_1(\mathbf{r}_1; t) & (63) \\ & + \rho_0^2 \int d^3r_2 (g_2(\mathbf{r}_1, \mathbf{r}_2) - 1) \delta u_2(\mathbf{r}_2; t) \\ & + \rho_0^2 \int d^3r_2 \left[ (g_2(\mathbf{r}_1, \mathbf{r}_2) \delta u_2(\mathbf{r}_1, \mathbf{r}_2; t) \right. \\ & \left. + \frac{\rho_0}{2} \int d^3r_3 (g_3(\mathbf{r}_1, \mathbf{r}_2, \mathbf{r}_3) - g_2(\mathbf{r}_2, \mathbf{r}_3)) \delta u_2(\mathbf{r}_2, \mathbf{r}_3; t) \right] \end{aligned}$$



From the definition (56) one sees directly that the **particle number is conserved** in the fluctuations

$$\int d^3r \delta\rho_1(\mathbf{r}) = 0 \quad (64)$$

and that the **sequential relation is satisfied**,

$$\int d^3r_2 \delta\rho_2(\mathbf{r}_1, \mathbf{r}_2; t) = (N-1)\delta\rho_1(\mathbf{r}_1; t) \quad (65)$$

The **one- and two-particle currents** are

$$\begin{aligned} \mathbf{j}_1(\mathbf{r}_1; t) &= \frac{\hbar\rho_0}{2mi} \left\{ \nabla_1 \delta u_1(\mathbf{r}_1; t) \right. \\ &\quad \left. + \rho_0 \int d^3r_2 g_2(\mathbf{r}_1, \mathbf{r}_2) \nabla_1 \delta u_2(\mathbf{r}_1, \mathbf{r}_2; t) \right\} \\ \mathbf{j}_2(\mathbf{r}_1, \mathbf{r}_2; t) &= \frac{\hbar\rho_0^2}{2mi} \left\{ g_2(\mathbf{r}_1, \mathbf{r}_2) [\nabla_1 \delta u_1(\mathbf{r}_1; t) \right. \\ &\quad \left. + \nabla_1 \delta u_2(\mathbf{r}_1, \mathbf{r}_2; t)] \right. \\ &\quad \left. + \rho_0 \int d^3r_3 g_3(\mathbf{r}_1, \mathbf{r}_2, \mathbf{r}_3) \nabla_1 \delta u_2(\mathbf{r}_1, \mathbf{r}_3; t) \right\}. \end{aligned} \quad (66)$$

The currents also satisfy the **sequential condition**

$$\int d^3r_2 \mathbf{j}_2(\mathbf{r}_1, \mathbf{r}_2; t) = (N-1) \mathbf{j}_1(\mathbf{r}_1; t). \quad (68)$$

The terms which depend on the **external potential** are collected into the functions  $D_1(\mathbf{r}_1; t)$  and  $D_2(\mathbf{r}_1, \mathbf{r}_2; t)$  and they drive excitations into the system

$$\begin{aligned} D_1(\mathbf{r}_1; t) &= \frac{2\rho_0}{\hbar} \left\{ U_{\text{ext}}(\mathbf{r}_1; t) \right. \\ &\quad \left. + \rho_0 \int d^3r_2 [g_2(\mathbf{r}_1, \mathbf{r}_2) - 1] U_{\text{ext}}(\mathbf{r}_2; t) \right\} \end{aligned} \quad (69)$$

$$\begin{aligned} D_2(\mathbf{r}_1, \mathbf{r}_2; t) &= \frac{2\rho_0^2}{\hbar} \left\{ g_2(\mathbf{r}_1, \mathbf{r}_2) [U_{\text{ext}}(\mathbf{r}_1; t) + U_{\text{ext}}(\mathbf{r}_2; t)] \right. \\ &\quad \left. + \rho_0 \int d^3r_3 [g_3(\mathbf{r}_1, \mathbf{r}_2, \mathbf{r}_3) - g_2(\mathbf{r}_1, \mathbf{r}_2)] U_{\text{ext}}(\mathbf{r}_3; t) \right\}. \end{aligned} \quad (70)$$

## 4 Solving the continuity equations

Up to now, we have formulated the problem in terms of a Hamiltonian, a trial wave function, and the action principle. What we still need to do is to find a

way to actually solve the continuity equations. They still contain four unknown quantities, namely  $\delta u_1(\mathbf{r}; t)$  and  $\delta u_2(\mathbf{r}_1, \mathbf{r}_2; t)$  and time derivatives of  $\delta \rho_1(\mathbf{r}; t)$  and  $\delta \rho_2(\mathbf{r}_1, \mathbf{r}_2; t)$ . Assuming that all ground state quantities are known. Clearly they are not independent, but connected by the definition (56). In the following we introduce various approximation schemas to put that definition into solving the continuity equations.

In the homogeneous system fluctuations are weak and it is more convenient to work in the **Fourier space**. We define the one-particle Fourier transform as

$$\begin{aligned}\delta \tilde{u}_1(\mathbf{k}; \omega) &= \rho_0 \int d^3 r dt e^{i(\mathbf{k}\cdot\mathbf{r}-\omega t)} \delta u_1(\mathbf{r}; t) \\ \delta u_1(\mathbf{r}; t) &= \int \frac{d^3 k d\omega}{(2\pi)^4 \rho_0} e^{-i(\mathbf{k}\cdot\mathbf{r}-\omega t)} \delta \tilde{u}_1(\mathbf{k}; \omega)\end{aligned}$$

and similarly for the two-particle Fourier transforms

$$\begin{aligned}\mathcal{F}[f(\mathbf{r}_1, \mathbf{r}_2; t)] &= \rho_0^2 \int d^3 r_1 d^3 r_2 dt e^{i(\mathbf{k}\cdot\mathbf{R}+\mathbf{p}\cdot\mathbf{r}-\omega t)} f(\mathbf{r}_1, \mathbf{r}_2; t) \\ \mathcal{F}^{-1}[\tilde{f}(\mathbf{k}, \mathbf{p}; t)] &= \int \frac{d^3 k d^3 p d\omega}{(2\pi)^7 \rho_0^2} e^{-i(\mathbf{k}\cdot\mathbf{R}+\mathbf{p}\cdot\mathbf{r}-\omega t)} \tilde{f}(\mathbf{k}, \mathbf{p}; \omega)\end{aligned}$$

where  $\mathbf{R} = (\mathbf{r}_1 + \mathbf{r}_2)/2$  is the center-of-mass vector, and  $\mathbf{r} = \mathbf{r}_1 - \mathbf{r}_2$  the relative position vector.

#### 4.1 Feynman approximation

Let us first calculate the simplest approximation where we let only the one-particle correlation function vary with time. This leads to the Feynman result for excitations.

We need to solve the first continuity equation (61) in momentum space with the assumption  $\delta u_2(\mathbf{r}_1, \mathbf{r}_2; t) = 0$  Then the current is simply

$$\mathbf{j}_1(\mathbf{r}_1; t) = \frac{\hbar \rho_0}{2mi} \nabla_1 \delta u_1(\mathbf{r}_1; t) \quad (71)$$

and the time dependent part of the density

$$\begin{aligned}\delta \rho_1(\mathbf{r}_1; t) &= \rho_0 \delta u_1(\mathbf{r}_1; t) \\ &+ \rho_0^2 \int d^3 r_2 h(\mathbf{r}_1, \mathbf{r}_2) \delta u_1(\mathbf{r}_2; t)\end{aligned} \quad (72)$$

with  $h(\mathbf{r}_1, \mathbf{r}_2) \equiv g_2(\mathbf{r}_1, \mathbf{r}_2) - 1$ . The Fourier transforms can be readily calculated giving

$$\delta \tilde{\rho}_1(\mathbf{k}; \omega) = S(k) \rho_0 \delta \tilde{u}_1(\mathbf{k}; \omega) \quad (73)$$

and then

$$\delta \tilde{u}_1(\mathbf{k}; \omega) = \frac{1}{\rho_0 S(k)} \delta \tilde{\rho}_1(\mathbf{k}; \omega) \quad (74)$$

Similarly we can calculate the Fourier transform of the contribution from the external potential (69). Inserting these results into the continuity equation (61) we get

$$-\frac{\hbar k^2}{2mS(k)}\delta\tilde{\rho}_1(\mathbf{k};\omega) + \omega\delta\tilde{\rho}_1(\mathbf{k};\omega) = \frac{2\rho_0}{\hbar}S(\mathbf{k})U_{\text{ext}}(k,\omega) \quad (75)$$

and we can solve the linear response function

$$\chi(k,\omega) = \frac{\delta\tilde{\rho}_1(\mathbf{k};\omega)}{\rho_0 U_{\text{ext}}(k,\omega)} = \frac{2S(k)}{\hbar\omega - \frac{\hbar^2 k^2}{2mS(k)}} \quad (76)$$

The poles of  $\chi(k,\omega)$  give the elementary excitations of the system

$$\varepsilon_F(k) = \hbar\omega = \frac{\hbar^2 k^2}{2mS(k)} \quad (77)$$

and the limit  $\omega = 0$  the static response function

$$\chi(k,0) = -\frac{4mS^2(k)}{\hbar^2 k^2} \quad (78)$$

The imaginary part of the linear response function determines the dynamic structure function (33)

$$S(k,\omega) = -\frac{1}{2\pi}\Im[\chi(k,\omega)] = S(k)\delta(\hbar\omega - \varepsilon_F(k)) \quad (79)$$

which means that the Feynman approximation is a single pole approximation and the strength of the pole is the structure function.

In  $^4\text{He}$  the excitation mode is linear in the long wave length limit and proportional to the speed of sound  $c$ ,

$$\varepsilon_F \rightarrow \hbar kc. \quad (80)$$

The structure function is also linear at small  $k$

$$S(k) \rightarrow \frac{\hbar k}{2mc} \quad (81)$$

and the inverse of the static response function determines the incompressibility

$$-\chi^{-1}(k,0) \rightarrow mc^2 \quad (82)$$

The elementary excitation modes of the system are obtained also directly by setting the external potential  $U_{\text{ext}} = 0$  in the continuity equations. Using the Feynman approximation and the results (71) and (72) we get a differential equation

$$\begin{aligned} & \frac{\hbar\rho_0}{2mi}\nabla_1^2\delta u_1(\mathbf{r}_1;\omega) - i\omega\left[\rho_0\delta u_1(\mathbf{r}_1;\omega) \right. \\ & \left. + \rho_0^2\int d^3r_2 h(\mathbf{r}_1,\mathbf{r}_2)\delta u_1(\mathbf{r}_2;\omega)\right] = 0 \end{aligned} \quad (83)$$

which has the solution (77) and

$$\delta u_1(\mathbf{r}_1; \omega) = e^{i\mathbf{k}\cdot\mathbf{r}_1} \quad (84)$$

The excitation operator has then the Feynman form

$$\delta U = \sum_j \delta u_1(\mathbf{r}_j; \omega) = \sum_j e^{i\mathbf{k}\cdot\mathbf{r}_j} \quad (85)$$

## 5 CBF-approximation

When the two-particle correlation function is allowed to vary with time then the first continuity equations (61) can be written in momentum space in a general form

$$\hbar\omega - \varepsilon_F(k) - \Sigma(k, \omega) = 2S(k)\chi^{-1}(k, \omega). \quad (86)$$

where  $\Sigma(k, \omega)$  is the **self energy** and the linear response function as

$$\chi(k, \omega) = \frac{2S(k)}{\hbar\omega - \varepsilon_F(k) - \Sigma(k, \omega)} \quad (87)$$

For real values of the self-energy the response function can have poles which define the collective, elementary excitations. When the decay of the excited modes becomes possible then the self-energy acquires imaginary part and the sharp  $\delta$ -function in the imaginary part of the response function spreads into a broader peak. The notation  $\varepsilon_F(k)$  stands for the energy of the Feynman collective mode.

### 5.1 Convolution approximation

The derivation of the self-energy starts [29, 33] with a convolution approximation of the **three-particle distribution function**, but including also a special set of diagrams with the triplet correlation function  $u_3(\mathbf{r}_1, \mathbf{r}_2, \mathbf{r}_3)$ . The terms included are shown in Fig. 1.

In the algebraic form it becomes

$$\begin{aligned} g_3(\mathbf{r}_1, \mathbf{r}_2, \mathbf{r}_3) &= 1 + h(\mathbf{r}_1, \mathbf{r}_2) + h(\mathbf{r}_1, \mathbf{r}_3) + h(\mathbf{r}_2, \mathbf{r}_3) \\ &+ h(\mathbf{r}_1, \mathbf{r}_2)h(\mathbf{r}_1, \mathbf{r}_3) + h(\mathbf{r}_1, \mathbf{r}_2)h(\mathbf{r}_2, \mathbf{r}_3) \\ &+ h(\mathbf{r}_1, \mathbf{r}_3)h(\mathbf{r}_2, \mathbf{r}_3) + \int d^3r_4 h(\mathbf{r}_1, \mathbf{r}_4)h(\mathbf{r}_2, \mathbf{r}_4)h(\mathbf{r}_3, \mathbf{r}_4) \\ &+ \text{terms with triplet correlations functions} \end{aligned} \quad (88)$$

The Fourier transform of that is simply

$$\begin{aligned} \mathcal{F}[g_3(\mathbf{r}_1, \mathbf{r}_2, \mathbf{r}_3) - 1] &= S(\mathbf{k}_1)S(\mathbf{k}_2)S(\mathbf{k}_3) \\ &\times [1 + u_3(\mathbf{k}_1, \mathbf{k}_2, \mathbf{k}_3)] - 1 \end{aligned} \quad (89)$$

We ignore triplet correlations for a moment and return to them at the end of this section.

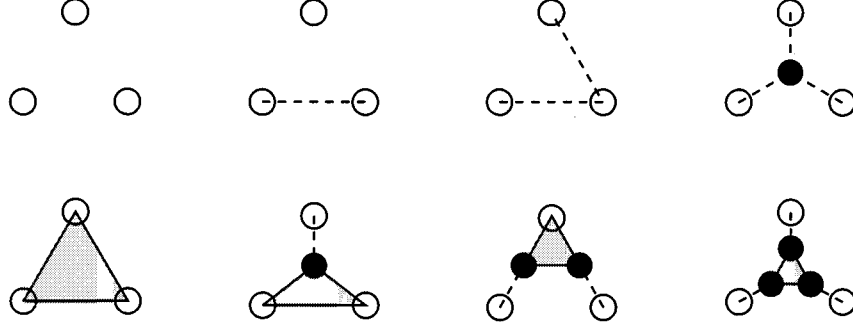


Figure 1: Convolution approximation of  $g_3(\mathbf{r}_1, \mathbf{r}_2, \mathbf{r}_3)$ . Circles are particle positions, black circles are integrated and open circles not. Dashed lines are functions  $h(\mathbf{r}_1, \mathbf{r}_2)$  and triangles are triplet correlation functions  $u_3(\mathbf{r}_1, \mathbf{r}_2, \mathbf{r}_3)$ . The second, third fifth and sixth diagrams have three of the same kind, but with different particle coordinates.

## 5.2 Two-particle equation

Our aim is to get an approximation for  $\delta u_2(\mathbf{r}_1, \mathbf{r}_2; t)$  using Eq.(62). The simplest term to approximate is  $D_2(\mathbf{r}_1, \mathbf{r}_2; t)$  in Eq. (70)

$$\begin{aligned}
 D_2(\mathbf{r}_1, \mathbf{r}_2; t) &= \frac{2\rho_0^2}{\hbar} \left\{ g_2(\mathbf{r}_1, \mathbf{r}_2) (D_1(\mathbf{r}_1; t) + D_1(\mathbf{r}_2; t)) \right. \\
 &+ \rho_0 \int d^3 r_3 U_{\text{ext}}(\mathbf{r}_3; t) \\
 &\times \left[ h(\mathbf{r}_1, \mathbf{r}_3)h(\mathbf{r}_2, \mathbf{r}_3) + \int h(\mathbf{r}_1, \mathbf{r}_4)h(\mathbf{r}_2, \mathbf{r}_4)h(\mathbf{r}_3, \mathbf{r}_4) \right] \left. \right\}. \tag{90}
 \end{aligned}$$

The last two lines can be written in the form

$$\rho_0 \int d^3 r_3 Y(\mathbf{r}_1, \mathbf{r}_2; \mathbf{r}_3) D_1(\mathbf{r}_3; t) \tag{91}$$

with  $Y(\mathbf{r}_1, \mathbf{r}_2; \mathbf{r}_3) = h(\mathbf{r}_1, \mathbf{r}_3)h(\mathbf{r}_2, \mathbf{r}_3)$ . The triplet correlation will have additional contribution to that. Thus we can express the **two particle driving** term entirely in terms of  $D_1(\mathbf{r}; t)$ .

$$\begin{aligned}
 D_2(\mathbf{r}_1, \mathbf{r}_2; t) &= \frac{2\rho_0^2}{\hbar} \left\{ g_2(\mathbf{r}_1, \mathbf{r}_2) (D_1(\mathbf{r}_1; t) + D_1(\mathbf{r}_2; t)) \right. \\
 &+ \left. \rho_0 \int d^3 r_3 Y(\mathbf{r}_1, \mathbf{r}_2; \mathbf{r}_3) D_1(\mathbf{r}_3; t) \right\} \tag{92}
 \end{aligned}$$

Similarly we can write an expression for the time dependent **two-particle density** using Eqs. (56) and (63)

$$\delta \rho_2(\mathbf{r}_1, \mathbf{r}_2; t) = \rho_0 \left\{ g_2(\mathbf{r}_1, \mathbf{r}_2) (\delta \rho_1(\mathbf{r}_1; t) + \delta \rho_1(\mathbf{r}_2; t)) \right.$$

$$\begin{aligned}
& + \rho_0 \int d^3 r_3 Y(\mathbf{r}_1, \mathbf{r}_2; \mathbf{r}_3) \delta \rho_1(\mathbf{r}_3; t) \Big\} \\
& + \rho_0^2 g_2(\mathbf{r}_1, \mathbf{r}_2) \delta u_2(\mathbf{r}_1, \mathbf{r}_2; t) + \mathcal{F}[\delta u_2]
\end{aligned} \tag{93}$$

We have removed the dependence on  $\delta u_1(\mathbf{r}, t)$  in favor of  $\delta \rho_1(\mathbf{r}, t)$ . The functional  $\mathcal{F}[\delta u_2]$  contains all the rest of the terms with  $\delta u_2(\mathbf{r}_1, \mathbf{r}_2; t)$ . They can be written explicitly using the definition (56), but they are not included in the CBF-approximation.

The **two particle current** has a term with one-particle current, but also structure which comes from the time-dependent two-particle correlations.

$$\begin{aligned}
\mathbf{j}_2(\mathbf{r}_1, \mathbf{r}_2; t) & = \rho_0 g_2(\mathbf{r}_1, \mathbf{r}_2) \mathbf{j}_1(\mathbf{r}_1) \\
& + \frac{\hbar \rho_0^2}{2mi} \left\{ g_2(\mathbf{r}_1, \mathbf{r}_2) \nabla_1 \delta u_2(\mathbf{r}_1, \mathbf{r}_2; t) + \rho_0 \int d^3 r_3 \right. \\
& \times \left. [g_3(\mathbf{r}_1, \mathbf{r}_2, \mathbf{r}_3) - g_2(\mathbf{r}_1, \mathbf{r}_2) g_2(\mathbf{r}_1, \mathbf{r}_3)] \nabla_1 \delta u_2(\mathbf{r}_1, \mathbf{r}_3) \right\}
\end{aligned} \tag{94}$$

The final steps of the derivation are the approximations necessary to bring the two-body equation in a numerically tractable form. Our scheme follows the general strategy of the **uniform limit approximation** [6] which has been quite successful for the calculation of the optimal static three-body correlations [34, 35, 36]. The essence of the approximation is to consider **all products of two or more two-body functions small in coordinate space**.

In our specific case, the uniform limit approximation amounts to taking  $g_2(\mathbf{r}_1, \mathbf{r}_2) \delta u_2(\mathbf{r}_1, \mathbf{r}_2) \approx \delta u_2(\mathbf{r}_1, \mathbf{r}_2)$  and a similar expression for  $\nabla_1 \delta u_2(\mathbf{r}_1, \mathbf{r}_2)$ . While this approximation places more emphasis on the structure of  $\delta u_2(\mathbf{r}_1, \mathbf{r}_2)$  it is physically appealing since it simply removes the *redundant* relevant short-range structure shared by  $g_2(\mathbf{r}_1, \mathbf{r}_2)$  and  $\delta u_2(\mathbf{r}_1, \mathbf{r}_2)$ . Invoking the equivalent uniform limit for the three-body distribution function, the terms in Eq. (94) which depend on  $\delta u_2(\mathbf{r}_1, \mathbf{r}_2)$  become

$$\begin{aligned}
& \frac{\hbar \rho_0^2}{2mi} \left[ g_2(\mathbf{r}_1, \mathbf{r}_2) \nabla_1 \delta u_2(\mathbf{r}_1, \mathbf{r}_2) + \rho_0 \int d^3 r_3 \right. \\
& \times \left. [g_3(\mathbf{r}_1, \mathbf{r}_2, \mathbf{r}_3) - g_2(\mathbf{r}_1, \mathbf{r}_3) g_2(\mathbf{r}_1, \mathbf{r}_2)] \nabla_1 \delta u_2(\mathbf{r}_1, \mathbf{r}_3) \right] \\
& \approx \frac{\hbar \rho_0}{2mi} \int d^3 r_3 [\delta(\mathbf{r}_3 - \mathbf{r}_2) + h(\mathbf{r}_3, \mathbf{r}_2)] \nabla_1 \delta u_2(\mathbf{r}_1, \mathbf{r}_3).
\end{aligned}$$

We can now put together the approximate **two-particle continuity equation**

$$\begin{aligned}
& \nabla_1 \cdot \left[ g_2(\mathbf{r}_1, \mathbf{r}_2) \mathbf{j}_1(\mathbf{r}_1) \right. \\
& \left. + \frac{\hbar \rho_0}{2mi} \int d^3 r_3 [\delta(\mathbf{r}_3 - \mathbf{r}_2) + h(\mathbf{r}_3, \mathbf{r}_2)] \nabla_1 \delta u_2(\mathbf{r}_1, \mathbf{r}_3) \right]
\end{aligned}$$

$$\begin{aligned}
& + \text{ same with } (1 \leftrightarrow 2) \\
& = g_2(\mathbf{r}_1, \mathbf{r}_2) \left( \frac{2\rho_0}{\hbar} D_1(\mathbf{r}_1; t) - i\delta\dot{\rho}_1(\mathbf{r}_1; t) \right) \\
& + \frac{2\rho_0}{\hbar} D_1(\mathbf{r}_2; t) - i\delta\dot{\rho}_1(\mathbf{r}_2; t) \\
& + \rho_0 \int d^3r_3 Y(\mathbf{r}_1, \mathbf{r}_2; \mathbf{r}_3) \left( \frac{2\rho_0}{\hbar} D_1(\mathbf{r}_3; t) - i\delta\dot{\rho}_1(\mathbf{r}_3; t) \right) \\
& + \rho_0 \delta\dot{u}_2(\mathbf{r}_1, \mathbf{r}_2; t)
\end{aligned} \tag{95}$$

From the terms containing the time derivative  $\delta\dot{u}_2(\mathbf{r}_1, \mathbf{r}_2; t)$  we have kept only the leading term in accordance with the uniform limit approximation and left out the term  $\mathcal{F}[\delta\dot{u}_2]$ .

If we further more use the one-particle continuity equation to replace the one-particle quantities with one-particle currents we arrive at our final approximate form

$$\begin{aligned}
& \left[ \frac{\hbar\rho_0}{2mi} \int d^3r_3 [\delta(\mathbf{r}_3 - \mathbf{r}_2) + h(\mathbf{r}_3, \mathbf{r}_2)] \nabla_1^2 \delta u_2(\mathbf{r}_1, \mathbf{r}_3) \right. \\
& \left. + \text{same with } (1 \leftrightarrow 2) \right] - \delta\dot{u}_2(\mathbf{r}_1, \mathbf{r}_2; t) \\
& = \mathbf{j}_1(\mathbf{r}_1; t) \cdot \nabla_1 \cdot g_2(\mathbf{r}_1, \mathbf{r}_2) + \mathbf{j}_1(\mathbf{r}_2; t) \cdot \nabla_2 \cdot g_2(\mathbf{r}_1, \mathbf{r}_2) \\
& + \rho_0 \int d^3r_3 Y(\mathbf{r}_1, \mathbf{r}_2; \mathbf{r}_3) \nabla_3 \cdot \mathbf{j}_1(\mathbf{r}_3; t)
\end{aligned} \tag{96}$$

Approximating now the one-particle current (66) by the **Feynman current**

$$\begin{aligned}
\mathbf{j}(\mathbf{r}) & = \frac{\hbar\rho_0}{2mi} \nabla_1 \delta u_1(\mathbf{r}; t) \\
& = \frac{\hbar\rho_0}{2mi} \nabla_1 \left[ \delta\rho_1(\mathbf{r}_1; t) - \rho_0 \int d^3r_2 X(\mathbf{r}_1, \mathbf{r}_2) \delta\rho_1(\mathbf{r}_2; t) \right]
\end{aligned} \tag{97}$$

allows us to decouple the equations of motion. In other words the fluctuating two-point function can be expressed, in closed form, as a functional of one-body quantities alone.

Within this approximation the **second continuity equation** can be given in the form

$$\begin{aligned}
& [\hbar\omega - \varepsilon_F(|\frac{\mathbf{k}}{2} + \mathbf{p}|) - \varepsilon_F(|\frac{\mathbf{k}}{2} - \mathbf{p}|)] \\
& \times S(|\frac{\mathbf{k}}{2} + \mathbf{p}|) S(|\frac{\mathbf{k}}{2} - \mathbf{p}|) \delta u_2(\mathbf{k}, \mathbf{p}; \omega) \\
& + \varepsilon_F(k) \sigma_{\mathbf{k}}(\mathbf{p}) \delta\rho_1(\mathbf{k}; \omega) = 0.
\end{aligned} \tag{98}$$

Here  $\sigma_{\mathbf{k}}(\mathbf{p})$  corresponds to

$$\begin{aligned} \sigma_{\mathbf{k}}(\mathbf{p}) = & -\frac{1}{k^2} [\mathbf{k} \cdot (\frac{\mathbf{k}}{2} + \mathbf{p}) S(|\frac{\mathbf{k}}{2} - \mathbf{p}|) + (\mathbf{p} \leftrightarrow -\mathbf{p})] \\ & + S(|\frac{\mathbf{k}}{2} + \mathbf{p}|) S(|\frac{\mathbf{k}}{2} - \mathbf{p}|) [1 + \tilde{u}_3(\frac{\mathbf{k}}{2} + \mathbf{p}, \frac{\mathbf{k}}{2} - \mathbf{p}, -\mathbf{k})]. \end{aligned} \quad (99)$$

This is an algebraic equation from which we can solve the fluctuating **two-particle correlation function**,

$$\frac{\delta u_2(\mathbf{k}, \mathbf{p}; \omega)}{\delta \rho_1(\mathbf{k}; \omega)} = \frac{\varepsilon_F(k) \sigma_{\mathbf{k}}(\mathbf{p}) [S(|\frac{\mathbf{k}}{2} + \mathbf{p}|) S(|\frac{\mathbf{k}}{2} - \mathbf{p}|)]^{-1}}{\hbar\omega - \varepsilon_F(|\frac{\mathbf{k}}{2} + \mathbf{p}|) - \varepsilon_F(|\frac{\mathbf{k}}{2} - \mathbf{p}|)},$$

needed for the self energy.

### 5.3 One-particle equation

Let us now return to the **first continuity equation** (61) and to the one-particle current (66). We want again to remove  $\delta u_1(\mathbf{r}_1; t)$  in favor of  $\delta \rho_1(\mathbf{r}_1; t)$  within the convolution approximation. In that approximation the one-particle density (63) can be written in the form

$$\delta \rho_1(\mathbf{r}_1; t) = \rho_0 \delta v_1(\mathbf{r}_1; t) + \rho_0^2 \int d^3 r_2 h(\mathbf{r}_1, \mathbf{r}_2; t) \delta v_1(\mathbf{r}_2; t) \quad (100)$$

with

$$\begin{aligned} \delta v_1(\mathbf{r}_1; t) = & \delta u_1(\mathbf{r}_1; t) \\ & + \rho_0 \int d^3 r_2 g_2(\mathbf{r}_1, \mathbf{r}_2) \delta u_2(\mathbf{r}_1, \mathbf{r}_2; t) \\ & + \frac{1}{2} \rho_0^2 \int d^3 r_2 d^3 r_3 Y(\mathbf{r}_2, \mathbf{r}_3; \mathbf{r}_1) \delta u_2(\mathbf{r}_2, \mathbf{r}_3; t) \end{aligned} \quad (101)$$

Eq. (100) can be readily solved for  $\delta v_1(\mathbf{r}_1; t)$

$$\rho_0 \delta v_1(\mathbf{r}_1; t) = \delta \rho_1(\mathbf{r}_1; t) - \rho_0 \int d^3 r_2 X(\mathbf{r}_1, \mathbf{r}_2) \delta \rho_1(\mathbf{r}_2; t) \quad (102)$$

where  $X(\mathbf{r}_1, \mathbf{r}_2)$  is the direct correlation function.

From that we can solve the **one-particle correlation function**,

$$\begin{aligned} \rho_0 \delta u_1(\mathbf{r}_1; t) = & \delta \rho_1(\mathbf{r}_1; t) - \rho_0 \int d^3 r_2 X(\mathbf{r}_1, \mathbf{r}_2) \delta \rho_1(\mathbf{r}_2; t) \\ & - \rho_0^2 \int d^3 r_2 g_2(\mathbf{r}_1, \mathbf{r}_2) \delta u_2(\mathbf{r}_1, \mathbf{r}_2; t) \\ & - \frac{1}{2} \rho_0^3 \int d^3 r_2 d^3 r_3 Y(\mathbf{r}_2, \mathbf{r}_3; \mathbf{r}_1) \delta u_2(\mathbf{r}_2, \mathbf{r}_3; t) \end{aligned} \quad (103)$$



Taking its gradient and inserting into equation (66) we get the **one-particle current**

$$\begin{aligned} \mathbf{j}_1(\mathbf{r}_1; t) = & \nabla_1 \left[ \delta\rho_1(\mathbf{r}_1; t) - \rho_0 \int d^3r_2 X(\mathbf{r}_1, \mathbf{r}_2) \delta\rho_1(\mathbf{r}_2; t) \right] \\ & - \rho_0^2 \int d^3r_2 \delta u_2(\mathbf{r}_1, \mathbf{r}_2; t) \nabla_1 g_2(\mathbf{r}_1, \mathbf{r}_2) \\ & - \frac{1}{2} \rho_0^3 \int d^3r_2 d^3r_3 \nabla_1 Y(\mathbf{r}_1, \mathbf{r}_2, \mathbf{r}_3) \delta u_2(\mathbf{r}_2, \mathbf{r}_3; t) \end{aligned} \quad (104)$$

## 5.4 Self-energy

In momentum space the one-particle equation can now be written in the form

$$\begin{aligned} & [\hbar\omega - \varepsilon_F(k)] \delta\rho_1(\mathbf{k}; \omega) \\ & + \frac{\hbar^2 k^2}{4m} \int \frac{d^3p}{(2\pi)^3 \rho_0} \sigma_{\mathbf{k}}(\mathbf{p}) \delta u_2(\mathbf{k}, \mathbf{p}; \omega) = 2S(k) U_{ext}(k) \end{aligned} \quad (105)$$

where  $\sigma_{\mathbf{k}}(\mathbf{p})$  is the same as in the two-particle equation (99).

By dividing this equation with  $\delta\rho_1(\mathbf{k}; \omega)$  we get the self-energy and the inverse of the linear response function

$$\hbar\omega - \varepsilon_F(k) + \Sigma(\mathbf{k}, \omega) = 2S(k) \chi^{-1}(\mathbf{k}, \omega) \quad (106)$$

with

$$\Sigma(\mathbf{k}, \omega) = \frac{\hbar^2 k^2}{4m} \int \frac{d^3p}{(2\pi)^3 \rho_0} \sigma_{\mathbf{k}}(\mathbf{p}) \frac{\delta u_2(\mathbf{k}, \mathbf{p}; \omega)}{\delta\rho_1(\mathbf{k}; \omega)} \quad (107)$$

Let's change the variables  $\frac{\mathbf{k}}{2} + \mathbf{p} \rightarrow \mathbf{p}$  and  $\frac{\mathbf{k}}{2} - \mathbf{p} \rightarrow \mathbf{q}$  and then introduce the Dirac delta function to insure that  $\mathbf{p} + \mathbf{q} = \mathbf{k}$ . The self energy correction is written as

$$\Sigma^{\text{CBF}}(k, \omega) = \frac{1}{2} \int \frac{d^3p d^3q}{(2\pi)^3 \rho_0} \delta(\mathbf{k} + \mathbf{p} + \mathbf{q}) \frac{|V_3(\mathbf{k}; \mathbf{p}, \mathbf{q})|^2}{\hbar\omega - \varepsilon_F(p) - \varepsilon_F(q)}, \quad (108)$$

where the three-plasmon/phonon coupling matrix element

$$\begin{aligned} V_3(\mathbf{k}; \mathbf{p}, \mathbf{q}) &= \frac{\hbar^2}{2m} \frac{1}{\sqrt{S(p)S(q)S(k)}} \\ &\times \left[ -\mathbf{k} \cdot \mathbf{p} \tilde{S}(p) - \mathbf{k} \cdot \mathbf{q} \tilde{S}(q) + k^2 S(p) S(q) (1 + \tilde{u}_3(\mathbf{k}, \mathbf{p}, \mathbf{q})) \right] \\ &= \frac{\hbar^2}{2m} \sqrt{\frac{S(p)S(q)}{S(k)}} [\mathbf{k} \cdot \mathbf{p} \tilde{X}(p) + \mathbf{k} \cdot \mathbf{q} \tilde{X}(q) - k^2 \tilde{u}_3(\mathbf{k}, \mathbf{p}, \mathbf{q})]. \end{aligned} \quad (109)$$

is given in terms of the ground-state structure function  $S(k)$ , the direct correlation function  $\tilde{X}(k) = 1 - S(k)^{-1}$ , and the three-body correlation function  $\tilde{u}_3$ .

## 5.5 Numerical solution

The integrand (108) can have poles, which makes the self energy a complex function. Let us look next in detail how it is **calculated numerically**.

After integrating the  $\delta$ -function and the  $\phi$ -coordinate we are left with the double integral

$$\begin{aligned}\Sigma^{\text{CBF}}(k, \omega) &= \frac{1}{2} \frac{1}{(2\pi)^2 \rho_0} \int_0^\infty q^2 dq \int_{-1}^1 dx \\ &\times \frac{|V_3(k; q, x)|^2}{\hbar\omega - \varepsilon_{\text{F}}(|\mathbf{k} + \mathbf{q}|) - \varepsilon_{\text{F}}(q)},\end{aligned}$$

where we have chosen the following variables

$$\begin{aligned}\mathbf{p} &= -(\mathbf{k} + \mathbf{p}) \\ p^2 &= k^2 + 2\mathbf{k} \cdot \mathbf{q} = k^2 + q^2 + 2kpx \\ x &= \frac{p^2 - k^2 - q^2}{2kq}\end{aligned}\tag{110}$$

Replacing yet  $x$  with  $p$  we write the integral in the form

$$\begin{aligned}\Sigma^{\text{CBF}}(k, \omega) &= \frac{1}{8\pi^2 \rho_0 k} \int_0^\infty q dq \int_{|k-q|}^{k+q} p dp \\ &\times \frac{|V_3(k; q, p)|^2}{\hbar\omega - \varepsilon_{\text{F}}(p) - \varepsilon_{\text{F}}(q)},\end{aligned}\tag{111}$$

This integral has a pole when

$$\hbar\omega = \varepsilon_{\text{F}}(p) + \varepsilon_{\text{F}}(q)\tag{112}$$

In other words when the energy of the excitation is equal to the energy of two elementary Feynman modes. In such a case the self energy becomes a complex function. Assuming that this pole is the only pole in the integrand and that the integrand converges fast enough at infinity we can separate the real and imaginary parts

$$\Sigma(k, \omega) = \Delta(k, \omega) - i\Gamma(k, \omega)\tag{113}$$

by remembering that

$$\frac{1}{\omega' - \omega + i\eta} = \mathcal{P} \frac{1}{\omega' - \omega} - i\pi\delta(\omega' - \omega)\tag{114}$$

The **imaginary part** can then be calculated with one integration only

$$\begin{aligned}\Gamma(k, \omega) &= -\frac{1}{8\pi \rho_0 k} \int_0^\infty q dq \int_{|k-p|}^{k+p} p dp \\ &\times |V_3(k; q, p)|^2 \delta(\hbar\omega - \varepsilon_{\text{F}}(p) - \varepsilon_{\text{F}}(q))\end{aligned}\tag{115}$$

Figure 2: The dynamic structure function  $S(k, \omega)$  for three-dimensional liquid  ${}^4\text{He}$  in the CBF-approximation at the saturation density  $0.022 \text{ \AA}^{-3}$ .

The **real part** could be calculated from the above principle value integral, but it is much more convenient for numerics to calculate it from the imaginary part using **Kramers-Kronig relations** which connect the real and imaginary parts. If  $f(\omega)$  is an analytic complex function

$$f(\omega) = a(\omega) + ib(\omega) \quad (116)$$

then

$$\begin{aligned} a(\omega) &= \frac{1}{\pi} \mathcal{P} \int_{-\infty}^{\infty} d\omega' \frac{b(\omega')}{\omega' - \omega} \\ b(\omega) &= -\frac{1}{\pi} \mathcal{P} \int_{-\infty}^{\infty} d\omega' \frac{a(\omega')}{\omega' - \omega} \end{aligned} \quad (117)$$

Provided that  $a(\omega)$  and  $b(\omega)$  converge fast enough at large  $\omega$ .

Using the first relation we can write the real part of the self energy in the form

$$\Delta(k, \omega) = -\frac{1}{\pi} \mathcal{P} \int_0^{\infty} d\omega' \frac{\Gamma(k, \omega')}{\omega' - \omega} \quad (118)$$

The imaginary part is non-zero only when  $\omega' > 0$ . In the numerical integration of the principle value one distributes the integration mesh symmetrically around  $\omega$  and leaves out the point  $\omega' = \omega$ .

## 5.6 Analytic structure of the self-energy

The collective modes of the system are found by determining the poles (note that all poles are on the real axis[37]) of the response function (87), in other words by solving the implicit equation

$$\hbar\omega_0(k) = \varepsilon(k) + \Sigma(k, \omega_0(k)) \quad (119)$$

and the strength of the collective mode is given by

$$Z(k) = 2S(k) \left[ 1 - \frac{\partial}{\partial \omega} \Sigma(k, \omega) \Big|_{\omega=\omega_0(k)} \right]^{-1}. \quad (120)$$

From our definition (108) of the self-energy follows the inequality

$$\Sigma^{\text{CBF}}(k, \omega) \leq \Sigma^{\text{CBF}}(k, 0) \leq 0 \quad (121)$$

from which one immediately sees that the lowest collective mode satisfies the exact inequality [38]

$$\hbar\omega_0(k) \leq -\frac{2S(k)}{\chi^{\text{CBF}}(k, 0)}. \quad (122)$$

While it is reassuring that our microscopic approach satisfies known exact sum-rules and inequalities as a consequence of its structure, we will see momentarily that the inequality (122) is of rather limited use in determining features of either the excitation spectrum, or the static response function. The reason is that it gives *neither* information on the pole strength  $Z(k)$ , *nor* on the existence of stable collective modes. We shall encounter examples of both: a case where the pole strength of the lowest collective mode is infinitesimal, and a case where no real collective mode exists. The latter example is in fact a well-known consequence of anomalous dispersion.

In writing down Eq. (119) we have to assume that  $\Sigma(k, \omega_0(k))$  is real. This is the case when the energy denominator in Eq. (108) does not change sign, which is true when the collective energy is *below* the critical value

$$\hbar\omega_0 < \hbar\omega_{\text{crit}}(k) \equiv \min_{\mathbf{q}} [\varepsilon(\mathbf{q}) + \varepsilon(|\mathbf{k} + \mathbf{q}|)] \quad (123)$$

determining the continuum boundary. Above that energy, the self-energy is complex. Moreover, for  $\hbar\omega < \hbar\omega_{\text{crit}}(k)$ , it follows from Eq. (108) that

$$\frac{d\Sigma(k, \omega)}{d\omega} < 0 \quad \text{for} \quad \hbar\omega < \hbar\omega_{\text{crit}}(k). \quad (124)$$

In order to determine if Eq. (119) has a solution, we must find out whether  $\Sigma(k, \omega)$  becomes singular at the branch-cut  $\omega = \omega_{\text{crit}}(k)$  or not. This depends, of course, on the details of the reference spectrum  $\varepsilon(k)$  in the energy denominator of Eq. (119). We shall study here two relevant cases.

## 5.7 Anomalous dispersion in liquid $^4\text{He}$

**The first case** is that the reference spectrum  $\varepsilon(k)$  is **convex**. This refers typically to the regime of low momentum transfer in  $^4\text{He}$  where the sound mode has an **anomalous dispersion** or to high momentum transfer where the **spectrum approaches the single particle kinetic energy**. When  $\hbar\omega_{\text{crit}}(k) = 2\varepsilon(k/2) < \varepsilon(k)$ , this critical energy is *below* the reference energy. In order to determine whether Eq. (119) has a solution, we must therefore study the analytic behavior of  $\Sigma(k, \omega)$  as a function of  $\omega$  near the branch-point  $\omega = \omega_{\text{crit}}(k)$ . We shall treat only the simplest cases here, assuming a monotonically growing, convex spectrum  $\varepsilon'(k/2) > 0$  and  $\varepsilon''(k/2) > 0$  and we are interested in the singular behavior only.

As an example we evaluate the imaginary part of the integral (108) for  $\omega \approx \omega_{\text{crit}}$  for **two-dimensional  $^4\text{He}$** . [29] It is sufficient to consider the area where the

angle  $\theta$  between  $\mathbf{k}$  and  $\mathbf{q}$  is close to zero, i.e.

$$\Im m \Sigma(q, \omega) \approx -\frac{1}{2} \Im m \int \frac{d^2 k}{(2\pi)^2} \frac{|V(k, |k-q|, q)|^2}{\varepsilon_F(k) + \varepsilon_F(|\mathbf{k}-\mathbf{q}|) - \hbar\omega + i\eta}. \quad (125)$$

Next we expand the energy denominator in the vicinity of it's minimum value,  $\omega_{\text{crit}}(q)$ . Letting  $p = |\mathbf{k}-\mathbf{q}|$ , we have

$$\begin{aligned} & \varepsilon(k) + \varepsilon(p) \\ &= 2\varepsilon\left(\frac{q}{2}\right) + \varepsilon'(p+k-q) + \frac{1}{2}\varepsilon''\left(\left(k-\frac{q}{2}\right)^2 + \left(p-\frac{q}{2}\right)^2\right) \\ &= 2\varepsilon\left(\frac{q}{2}\right) + \frac{q}{2}\varepsilon''\left[\lambda(p+k-q) + \frac{1}{q}\left(k^2 + p^2 - \frac{q^2}{2}\right)\right] \end{aligned} \quad (126)$$

where

$$\varepsilon' = \left. \frac{d\varepsilon(q)}{dq} \right|_{\frac{q}{2}}, \quad \varepsilon'' = \left. \frac{d^2\varepsilon(q)}{dq^2} \right|_{\frac{q}{2}} \quad (127)$$

and

$$\lambda = \frac{2\varepsilon'}{k\varepsilon''} - 1. \quad (128)$$

For  $\cos\theta \approx 1$ , we can also expand (recall that we are considering momentum transfers  $k \approx \frac{q}{2}$ )

$$\begin{aligned} p &= \sqrt{k^2 + q^2 - 2kq + 2kq(1 - \cos\theta)} \\ &\approx q - k + \frac{kq}{(q-k)}(1 - \cos\theta) \\ &\approx q - k + (4k - q)(1 - \cos\theta) \end{aligned} \quad (129)$$

and therefore

$$\begin{aligned} \varepsilon(k) + \varepsilon(p) &= 2\varepsilon\left(\frac{q}{2}\right) + \frac{q^2\varepsilon''}{2}\left[\lambda\left(4\frac{k}{q} - 1\right)(1 - \cos\theta)\right. \\ &\quad \left. + \frac{2k}{q}\left(\frac{k}{q} - \cos\theta\right) + \frac{1}{2}\right]. \end{aligned} \quad (130)$$

This form of the energy denominator is correct, to **second order in the momentum, in the vicinity of it's minimum value and for small angles**. We can now carry out the angle integration and find

$$\begin{aligned} \Im m \Sigma(q, \omega) &\approx -\frac{1}{2} \Im m \int_0^\infty \frac{kdk}{(2\pi)^2} \int_0^{2\pi} d\theta \frac{|V(k, |k-q|, q)|^2}{A + B \cos\theta} \\ &= -\frac{1}{4\pi} \Im m \int_0^\infty kdk \frac{|V(k, |k-q|, q)|^2}{\hbar\sqrt{A^2 - B^2}} \end{aligned} \quad (131)$$

with

$$A = 2\varepsilon\left(\frac{q}{2}\right) + \frac{q^2\varepsilon''}{2} \left[ \lambda \left( 4\frac{k}{q} - 1 \right) + \frac{2k^2}{q^2} + \frac{1}{2} \right] - \omega + i\eta \quad (132)$$

and

$$B = -\frac{q^2\varepsilon''}{2} \left[ \lambda \left( 4\frac{k}{q} - 1 \right) + \frac{2k}{q} \right]. \quad (133)$$

For  $k \approx \frac{q}{2}$  and  $\omega \approx 2\varepsilon\left(\frac{q}{2}\right)$ , we can further simplify

$$A^2 - B^2 = 2k\varepsilon'\varepsilon''(k - k_-)(k - k_+) \quad (134)$$

with

$$k_{\pm} = \frac{q}{2} \pm \sqrt{\frac{\hbar\omega - 2\varepsilon(k/2)}{q^2\varepsilon''}}. \quad (135)$$

For  $\omega > 2\varepsilon(k/2)$  and  $k_- < k < k_+$ , the integrand is imaginary, and we get

$$\begin{aligned} \Im m \Sigma(q, \omega) &\approx \frac{|V(\frac{q}{2}, \frac{q}{2}, q)|^2}{4\pi} \\ &\times \int_{k_-}^{k_+} \frac{kdk}{\sqrt{2k\varepsilon'\varepsilon''(k - k_-)(k_+ - k)}} = q \frac{|V(\frac{q}{2}, \frac{q}{2}, q)|^2}{4\sqrt{2q\varepsilon'\varepsilon''}} \end{aligned} \quad (136)$$

whereas the imaginary part is zero for  $\omega < \omega_{\text{crit}}$ . With this, we have demonstrated that the imaginary part of the CBF self-energy has a finite discontinuity at  $\omega = \omega_{\text{crit}}$ . Analyticity arguments [39] are then sufficient to show (see Eq. (117)) that the real part must have a **logarithmic singularity** at the same place, and to determine the strength of that logarithmic singularity.

For the real part we get in 2D

$$\begin{aligned} &\lim_{\hbar\omega \rightarrow 2\varepsilon(k/2)} \Re e \Sigma^{\text{CBF}}(k, \omega) \\ &= \frac{|V_3(\mathbf{k}; -\mathbf{k}/2, -\mathbf{k}/2)|^2}{4\pi\rho_0} \frac{\ln(2\varepsilon(k/2) - \hbar\omega)}{\sqrt{2\varepsilon'(k/2)\varepsilon''(k/2)/k}} \end{aligned} \quad (137)$$

and in 3D

$$\begin{aligned} &\lim_{\hbar\omega \rightarrow 2\varepsilon(k/2)} \Re e \Sigma^{\text{CBF}}(k, \omega) \\ &= -\frac{|V_3(\mathbf{k}; -\mathbf{k}/2, -\mathbf{k}/2)|^2}{8\pi\rho_0} \frac{k\sqrt{2\varepsilon(k/2) - \hbar\omega}}{2\varepsilon'(k/2)\sqrt{\varepsilon''(k/2)}} \end{aligned} \quad (138)$$

Fig. 3 shows the CBF-BW self energy, for a low density two-dimensional case, as a function of momentum  $q$  and energy  $\hbar\omega$ . The logarithmic singularity at  $\omega = \omega_{\text{crit}}(q)$  is clearly seen, also that this singularity is, for low momenta, very sharp and permits under certain circumstances three solutions. These three

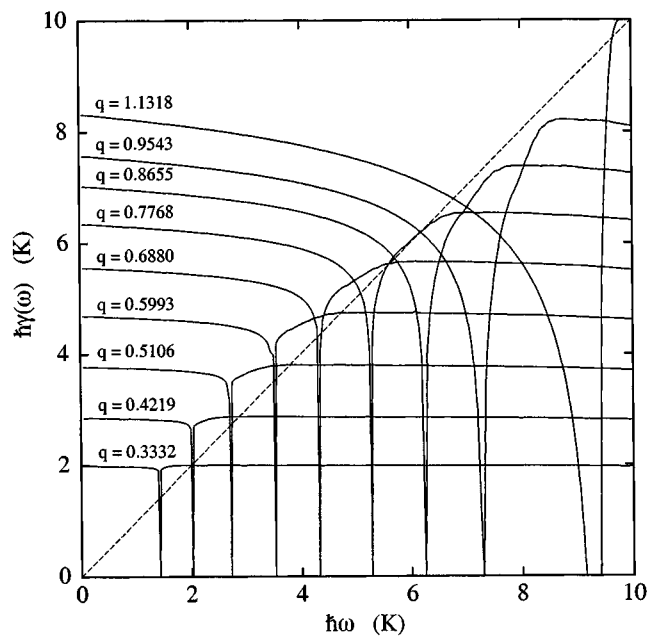


Figure 3: The CBF energy  $\gamma_q(\omega) = \varepsilon(q) + \Sigma(q, \omega)$  is shown, for two-dimensional  ${}^4\text{He}$ , as a function of  $\omega$  for a sequence of momentum values for  $n = 0.035 \text{ \AA}^{-2}$ . Solutions of the CBF-BW equations correspond to the points  $\gamma_q(\omega) = \omega$  along the dotted line. Clearly, for  $q < 0.77 \text{ \AA}^{-1}$  one has three solutions. It is also clearly seen that the logarithmic singularity is extremely narrow at small momenta.

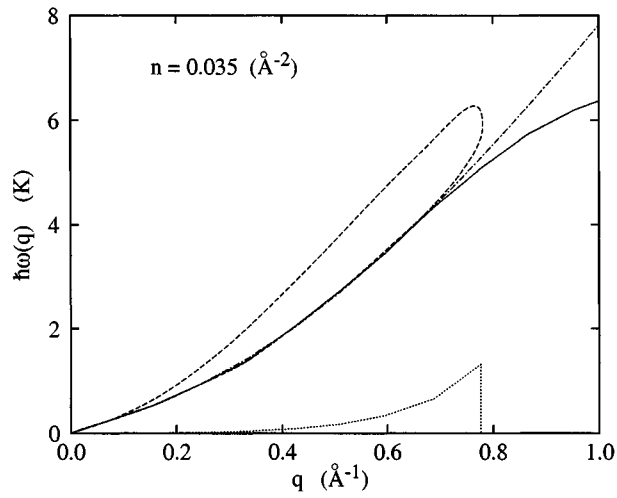


Figure 4: The three long-wavelength “solutions” of the CBF-BW equation in two-dimensional  ${}^4\text{He}$  for  $n = 0.035 \text{ \AA}^{-2}$ . The solid line is the lowest solution of the CBF-BW equation, the dashed loop the two solutions above  $\hbar\omega_{\text{crit}}(q)$  (dash-dotted line) and the dotted line at the bottom of the figure is the imaginary part of the highest solution.



Figure 5: The normalized dynamic structure function  $S(k, \omega)/S(k)$  is shown, for the 3D charged-boson gas, at  $r_s = 10$ . The strength of  $S(k, \omega)/S(k)$  is indicated by the greyscale. Also shown are the Feynman dispersion relations  $\varepsilon(k)$ , (long-dashed line), the self-energy corrected dispersion relation (solid line), and the continuum boundaries  $\hbar\omega_{\text{crit}}(k)$  (dotted line). The scale on the right refers to the *relative weight*  $Z(k)/S(k)$  (dotted line) and  $2m\omega_0(k)Z(k)/(\hbar k^2)$  (dash-dotted line) of the collective mode to the  $\omega^0$  and  $\omega^1$  sumrules

Figure 6: Same as Fig. 5 for 3D and  $r_s = 50$ .

solutions are shown in Fig. 4. There, the dash-dotted line is the boundary  $\hbar\omega_{\text{crit}}(k)$  above which all solutions are complex, and the dashed loop is the solution of the *real part* of the CBF-BW equation. It is also clearly seen that the *imaginary* part of the complex solution peaks just before the “mode” disappears.

The comparison between the two- and the three-dimensional cases is quite interesting. The self-energy is monotonically decreasing (*cf.* Eq. (124)) and has in two dimensions a logarithmic singularity at the branch-point, which guarantees that the dispersion relation (119) always has a real solution below the Feynman spectrum. In three dimensions, however, the self-energy remains *finite* at the branch-cut and, hence, the existence of a discrete collective excitation can no longer be guaranteed.

## 5.8 Absolute minimum in the spectrum

The second relevant case is when the reference spectrum has an absolute minimum. This is the case of the three-dimensional plasmon spectrum. In view of the further discussions, and due to its similarity to the case of  ${}^4\text{He}$ , we shall refer to this minimum as to the “roton minimum”. In this case, we have  $\omega_{\text{crit}}(k) = 2\omega_r$ , where  $\hbar\omega_r$  is the “roton energy” located at the wave number  $k_r$ . Expanding the energy denominator about this point yields the result

$$\lim_{\hbar\omega \rightarrow 2\hbar\omega_r} \Re \Sigma^{\text{CBF}}(k, \omega) = \frac{|V_3(\mathbf{k}; -\mathbf{k} - \mathbf{k}_r, \mathbf{k}_r)|^2}{8\pi\rho_0} \times \frac{k_r^2 \ln(2\hbar\omega_r - \hbar\omega)}{k\varepsilon''(k_r)}, \quad (139)$$

where  $\mathbf{k}_r$  is a vector of length  $k_r$  oriented such that the three vectors  $\mathbf{k}$ ,  $-\mathbf{k} - \mathbf{k}_r$ , and  $\mathbf{k}_r$  form an isosceles triangle. In two dimensions, one finds similarly a logarithmic singularity.

Figure 7: Same as Fig. 5 for 3D and  $r_s = 100$ .

To summarize the analysis of this section, we find that we can typically guarantee the existence of collective excitations in the *long-wavelength* regime in both two and three dimensions. An upper bound for these excitations is the Feynman spectrum or the continuum boundary  $\hbar\omega_{\text{crit}}(k)$ , whichever is lower. We have shown that, when the spectrum has a roton like structure, one can have collective excitations, even in the long-wavelength limit, *below the plasma frequency*, whereas the plasmon itself can decay for all finite, but infinitesimal wave numbers.

The numerical value of the strength  $Z(k)$  of the additional collective mode below the plasmon depends strongly on “how close” the solution of the implicit equation (119) is to the critical energy  $2\hbar\omega_p$ . For long wavelengths, the combination of Eqs. (109) and (139) yields for the self-energy

$$\begin{aligned} \Sigma^{\text{CBF}}(k, \omega) &= Ck \ln(2\hbar\omega_r - \hbar\omega) \\ \text{as } k \rightarrow 0+ \quad \text{and } \omega \nearrow 2\omega_r, \end{aligned} \quad (140)$$

where  $C$  is a numerical constant determined by the three phonon matrix element (109) and the kinematic factors appearing in Eq. (139). Note that the limits  $k \rightarrow 0+$  and  $\omega \nearrow 2\omega_r$  do not commute, here we must take the limit  $\omega \nearrow 2\omega_r$  first for fixed wave number and then evaluate the matrix elements in Eq. (139) for small  $k$ .

As a consequence, we obtain an energy for that “mode” of the order  $\hbar\omega = 2\hbar\omega_r - \text{const} \times \exp[\hbar(2\omega_r - \omega_p)/Ck]$  and a strength  $Z(k)$  that goes to zero as  $\exp[\hbar(2\omega_r - \omega_p)/Ck]$  for small  $k$ . Clearly this mode is a spurious solution of infinitesimal strength, but the very existence of that solution has, as we shall see, interesting consequences. Exact quantitative statements on the strength of that additional mode for *finite* wave numbers are difficult. We found that the strength of that additional mode is always small compared with the plasmon; the situation is generally very similar to that of  $^4\text{He}$  where we have discussed the analytic structure of the self-energy at length [29, 33].

The situation is different for high momentum transfers: the 3D self-energy remains *finite* at the branch-cut, *cf.* Eq. (138). This means that the existence of collective excitations can no longer be proven.

## 6 The full solution

Let us return to the definition of the density (56) and calculate the general expressions for the **gradients of the one and two-particle densities**,

$$\nabla_1 \delta\rho_1(\mathbf{r}_1; t) = \rho_0 \nabla_1 \delta u_1(\mathbf{r}_1; t) \quad (141)$$

$$\begin{aligned}
& + \rho_0^2 \int d^3 r_2 g_2(\mathbf{r}_1, \mathbf{r}_2) \nabla_1 \delta u_2(\mathbf{r}_1, \mathbf{r}_2; t) \\
& + \int d^3 r_2 \delta \rho_2(\mathbf{r}_1, \mathbf{r}_2; t) \nabla_1 u_2(\mathbf{r}_1, \mathbf{r}_2)
\end{aligned}$$

and

$$\begin{aligned}
& \nabla_1 \delta \rho_2(\mathbf{r}_1, \mathbf{r}_2; t) = \delta \rho_2(\mathbf{r}_1, \mathbf{r}_2; t) \nabla_1 u_2(\mathbf{r}_1, \mathbf{r}_2) \\
& + \rho_0 g_2(\mathbf{r}_1, \mathbf{r}_2) \nabla_1 [\delta u_1(\mathbf{r}_1; t) + \delta u_2(\mathbf{r}_1, \mathbf{r}_2; t)] \\
& + \rho_0^3 \int d^3 r_3 g_3(\mathbf{r}_1, \mathbf{r}_2, \mathbf{r}_3) \nabla_1 \delta u_2(\mathbf{r}_1, \mathbf{r}_3; t) \\
& + \int d^3 r_3 \delta \rho_3(\mathbf{r}_1, \mathbf{r}_2, \mathbf{r}_3; t) \nabla_1 u_2(\mathbf{r}_1, \mathbf{r}_3)
\end{aligned} \tag{142}$$

Here, we have assumed that also the ground state contains only the pair correlation function.

## 6.1 Continuity equations

Those terms which depend on  $\delta u_1(\mathbf{r}; t)$  and  $\delta u_2(\mathbf{r}_1, \mathbf{r}_2; t)$  in Eqs. (141) and (142) appear also in the expressions for the one- and two-body currents in Eqs. (66). Thus we can eliminate them and write the **currents** solely in terms of fluctuating densities.

$$\begin{aligned}
\mathbf{j}_1(\mathbf{r}_1; t) & = \frac{\hbar}{2mi} [\nabla_1 \delta \rho_1(\mathbf{r}_1; t) \\
& - \int d^3 r_2 \delta \rho_2(\mathbf{r}_1, \mathbf{r}_2; t) \nabla u_2(\mathbf{r}_1, \mathbf{r}_2)]
\end{aligned} \tag{143}$$

$$\begin{aligned}
\mathbf{j}_2(\mathbf{r}_1, \mathbf{r}_2; t) & = \frac{\hbar}{2mi} [\nabla_1 \delta \rho_2(\mathbf{r}_1, \mathbf{r}_2; t) \\
& - \delta \rho_2(\mathbf{r}_1, \mathbf{r}_2; t) \nabla_1 u_2(\mathbf{r}_1, \mathbf{r}_2) \\
& - \int d^3 r_3 \delta \rho_3(\mathbf{r}_1, \mathbf{r}_2, \mathbf{r}_3; t) \nabla_1 u_2(\mathbf{r}_1, \mathbf{r}_3)] .
\end{aligned} \tag{144}$$

Eq. (144) contains the three-body density variation,  $\delta \rho_3(\mathbf{r}_1, \mathbf{r}_2, \mathbf{r}_3; t)$  which must be formulated in terms of one- and two-particle density fluctuations.

Without loosing generality we can write the **density fluctuations** in terms of relative changes

$$\begin{aligned}
\delta \rho_1(\mathbf{r}_1; t) & = \rho_0 \xi(\mathbf{r}_1; t) \\
\delta \rho_2(\mathbf{r}_1, \mathbf{r}_2; t) & = \rho_0^2 g_2(\mathbf{r}_1, \mathbf{r}_2; t) \\
& \quad \times \left[ \xi(\mathbf{r}_1; t) + \xi(\mathbf{r}_2; t) + \Delta(\mathbf{r}_1, \mathbf{r}_2; t) \right] \\
\delta \rho_3(\mathbf{r}_1, \mathbf{r}_2, \mathbf{r}_3; t) & = \rho_0^3 g_3(\mathbf{r}_1, \mathbf{r}_2, \mathbf{r}_3; t)
\end{aligned}$$

$$\begin{aligned}
& \times \left[ \xi(\mathbf{r}_1; t) + \xi(\mathbf{r}_2; t) + \xi(\mathbf{r}_3; t) \right. \\
& + \Delta(\mathbf{r}_1, \mathbf{r}_2; t) + \Delta(\mathbf{r}_1, \mathbf{r}_3; t) + \Delta(\mathbf{r}_2, \mathbf{r}_3; t) \\
& \left. + \Delta_3(\mathbf{r}_1, \mathbf{r}_2, \mathbf{r}_3; t) \right] \quad (145)
\end{aligned}$$

From the definition of the  $n$ -particle density (54) we can derive the **Born-Green-Yvon (BGY) equations** by applying the gradient operator

$$\begin{aligned}
& \nabla_1 g_2(\mathbf{r}_1, \mathbf{r}_2) = g_2(\mathbf{r}_1, \mathbf{r}_2) \nabla_1 u_2(\mathbf{r}_1, \mathbf{r}_2) \\
& + \rho_0 \int d^3 r_3 g_3(\mathbf{r}_1, \mathbf{r}_2, \mathbf{r}_3) \nabla_1 u_2(\mathbf{r}_1, \mathbf{r}_3) \quad (146)
\end{aligned}$$

and since our ground state is homogeneous gradient with respect to one particle density vanishes provided that

$$\rho_0 \int d^3 r_2 g_2(\mathbf{r}_1, \mathbf{r}_2) \nabla_1 u_2(\mathbf{r}_1, \mathbf{r}_2) = 0 \quad (147)$$

With these substitutions we get

$$\begin{aligned}
\mathbf{j}_1(\mathbf{r}_1; t) &= \frac{\hbar \rho_0}{2mi} \left\{ \nabla_1 \xi(\mathbf{r}_1; t) - \right. \\
& \left. \rho_0 \int d^3 r_2 g_2(\mathbf{r}_1, \mathbf{r}_2) [\xi(\mathbf{r}_2; t) + \Delta(\mathbf{r}_1, \mathbf{r}_2; t)] \nabla_1 u_2(\mathbf{r}_1, \mathbf{r}_2) \right\} \\
\mathbf{j}_2(\mathbf{r}_1, \mathbf{r}_2; t) &= \frac{\hbar \rho_0^2}{2mi} \left\{ g_2(\mathbf{r}_1, \mathbf{r}_2) \nabla_1 [\xi(\mathbf{r}_1; t) + \Delta(\mathbf{r}_1, \mathbf{r}_2; t)] \right. \\
& - \rho_0 \int d^3 r_3 g_3(\mathbf{r}_1, \mathbf{r}_2, \mathbf{r}_3) [\xi(\mathbf{r}_3; t) + \Delta(\mathbf{r}_1, \mathbf{r}_3; t) \\
& \left. + \Delta(\mathbf{r}_2, \mathbf{r}_3; t) + \Delta(\mathbf{r}_1, \mathbf{r}_2, \mathbf{r}_3; t)] \nabla_1 u_2(\mathbf{r}_1, \mathbf{r}_3) \right\}. \quad (149)
\end{aligned}$$

These results are exact within the assumption that the wave function contains only one- and two-particle correlations, but the currents contain now three unknown quantities. A natural truncation is to set  $\Delta(\mathbf{r}_1, \mathbf{r}_2, \mathbf{r}_3; t) = 0$  since we have so far ignored also the fluctuating three-particle correlation functions. That is consistent with making the superposition approximation for the triplet distribution function

$$g_3(\mathbf{r}_1, \mathbf{r}_2, \mathbf{r}_3) = g_2(\mathbf{r}_1, \mathbf{r}_2) g_2(\mathbf{r}_1, \mathbf{r}_3) g_2(\mathbf{r}_2, \mathbf{r}_3) \quad (150)$$

Let us simplify the notation slightly by setting  $\mathbf{V}(\mathbf{r}_1, \mathbf{r}_2) \equiv g_2(\mathbf{r}_1, \mathbf{r}_2) \nabla_1 u_2(\mathbf{r}_1, \mathbf{r}_2)$  That is a ground

state quantity and can be calculated using the HNC-equations. Inserting this into the **continuity equations** they can be written for  $\xi(\mathbf{r}; t)$  and  $\Delta(\mathbf{r}_1, \mathbf{r}_2; t)$

$$\begin{aligned} & \frac{\hbar}{2mi} \nabla_1 \left\{ \nabla_1 \xi(\mathbf{r}_1; t) - \rho_0 \int d^3 r_2 \mathbf{V}(\mathbf{r}_1, \mathbf{r}_2) \right. \\ & \left. \times [\xi(\mathbf{r}_2; t) + \Delta(\mathbf{r}_1, \mathbf{r}_2; t)] \right\} + i\xi(\mathbf{r}_1; t) = \frac{1}{\rho_0} D_1(\mathbf{r}_1; t) \end{aligned} \quad (151)$$

and

$$\begin{aligned} & \frac{\hbar}{2mi} \nabla_1 \left\{ h(\mathbf{r}_1, \mathbf{r}_2) \nabla_1 [\xi(\mathbf{r}_1; t) + \Delta(\mathbf{r}_1, \mathbf{r}_2; t)] \right. \\ & \nabla_1 \Delta(\mathbf{r}_1, \mathbf{r}_2; t) - \rho_0 \int d^3 r_3 \mathbf{V}(\mathbf{r}_1, \mathbf{r}_3) \\ & \left. \left\{ \Delta(\mathbf{r}_2, \mathbf{r}_3; t) + [h(\mathbf{r}_1, \mathbf{r}_2)h(\mathbf{r}_2, \mathbf{r}_3) + h(\mathbf{r}_1, \mathbf{r}_2) + h(\mathbf{r}_2, \mathbf{r}_3)] \right. \right. \\ & \left. \left. [\xi(\mathbf{r}_3; t) + \Delta(\mathbf{r}_1, \mathbf{r}_3; t) + \Delta(\mathbf{r}_2, \mathbf{r}_3; t)] \right\} \right\} \\ & + ih(\mathbf{r}_1, \mathbf{r}_2) [\dot{\xi}(\mathbf{r}_1; t) + \dot{\xi}(\mathbf{r}_2; t) + \dot{\Delta}(\mathbf{r}_1, \mathbf{r}_2; t)] + \dot{\Delta}(\mathbf{r}_1, \mathbf{r}_2; t) \\ & = D_2(\mathbf{r}_1, \mathbf{r}_2; t) - D_1(\mathbf{r}_1; t) - D_2(\mathbf{r}_1; t) \end{aligned} \quad (152)$$

## 6.2 Continuity equations in momentum space

The first of the continuity equations (151) can be written in momentum space in the same form as before

$$\hbar\omega - \varepsilon(k) - \Sigma(k, \omega) = 2S(k)\chi^{-1}(k, \omega), \quad (153)$$

but now the collective excitation mode  $\varepsilon(k)$  is not any more a bare Feynman mode, but it contains a correction term which becomes important around the roton region.

To see that we need to calculate the Fourier transform

$$Q(k) = \mathcal{F} \left[ \nabla_1^2 \xi(\mathbf{r}_1; t) - \rho_0 \int d^3 r_2 \nabla_1 \cdot \mathbf{V}(\mathbf{r}_1, \mathbf{r}_2) \xi(\mathbf{r}_2; t) \right] \quad (154)$$

From the HNC-equation

$$g_2(\mathbf{r}_1, \mathbf{r}_2) = e^{u_2(\mathbf{r}_1, \mathbf{r}_2) + N(\mathbf{r}_1, \mathbf{r}_2) + E(\mathbf{r}_1, \mathbf{r}_2)} \quad (155)$$

we get

$$\mathbf{V}(\mathbf{r}_1, \mathbf{r}_2) = g_2(\mathbf{r}_1, \mathbf{r}_2) \nabla_1 u_2(\mathbf{r}_1, \mathbf{r}_2) \quad (156)$$

$$\begin{aligned} & = \nabla_1 g_2(\mathbf{r}_1, \mathbf{r}_2) + g_2(\mathbf{r}_1, \mathbf{r}_2) (\nabla_1 N(\mathbf{r}_1, \mathbf{r}_2) + \nabla_1 E(\mathbf{r}_1, \mathbf{r}_2)) \\ & = \nabla_1 X(\mathbf{r}_1, \mathbf{r}_2) - \nabla_1 E(\mathbf{r}_1, \mathbf{r}_2) \\ & - h(\mathbf{r}_1, \mathbf{r}_2) (\nabla_1 N(\mathbf{r}_1, \mathbf{r}_2) + \nabla_1 E(\mathbf{r}_1, \mathbf{r}_2)) \end{aligned} \quad (157)$$

where  $N(\mathbf{r}_1, \mathbf{r}_2)$  is the sum of nodal diagrams,  $X(\mathbf{r}_1, \mathbf{r}_2)$  the direct correlation function and  $E(\mathbf{r}_1, \mathbf{r}_2)$  the sum of elementary diagrams.

The leading term in the long wavelength limit is Fourier transform of the direct correlation function

$$\mathcal{F}[X(r)] = 1 - \frac{1}{S(k)} \quad (158)$$

with the structure function  $S(k)$  of the fluid. The Fourier transform of  $Q(k)$  is then

$$Q(k) = k^2 \left( 1 - \frac{1}{S(k)} \right) + I(k), \quad (159)$$

where  $I(k)$  stands for the integral

$$I(k) = -k^2 E(k) - \int \frac{d^3q}{(2\pi)^3 \rho} \mathbf{k} \cdot \mathbf{q} [S(|\mathbf{k} - \mathbf{q}|) - 1] [N(q) + E(q)]. \quad (160)$$

This leads to the expression

$$\varepsilon(k) = \frac{\hbar^2 k^2}{2mS(k)} [1 - S(k)I(k)], \quad (161)$$

for the reference collective mode. The correction term  $S(k)I(k)$  to the Feynman energy is positive and therefore the correction lowers the reference energy.

Note that in case the three-body correlations are included one should add a term

$$\frac{\rho}{2} \int d^3r g_3(\mathbf{r}_1, \mathbf{r}_2, \mathbf{r}_3) \nabla_1 u_3(\mathbf{r}_1, \mathbf{r}_2, \mathbf{r}_3) \quad (162)$$

into elementary diagrams.

**The self energy**  $\Sigma(k, \omega)$  is given by the integral

$$\Sigma(k, \omega) = -\frac{\hbar^2}{2m} \int \frac{d^3p}{(2\pi)^3 \rho} \mathbf{k} \cdot \left( \frac{\mathbf{k}}{2} + \mathbf{p} \right) \bar{Q} \left( \left| \frac{\mathbf{k}}{2} + \mathbf{p} \right| \right) \frac{\Delta(\mathbf{k}, \mathbf{p}; \omega)}{\xi(\mathbf{k}; \omega)}. \quad (163)$$

where

$$\bar{Q}(k) = \frac{Q(k)}{k^2} \quad (164)$$

The fluctuations appearing in the integrand can be solved using the second continuity equation. The singularity structure of the self energy as well as the second continuity equation are made more explicit by introducing the following notation,

$$\beta_{\mathbf{k}, \omega}(\mathbf{p}) \equiv [\hbar\omega - \varepsilon \left( \left| \frac{\mathbf{k}}{2} + \mathbf{p} \right| \right) - \varepsilon \left( \left| \frac{\mathbf{k}}{2} - \mathbf{p} \right| \right)] \frac{\Delta(\mathbf{k}, \mathbf{p}; \omega)}{\xi(\mathbf{k}; \omega)}$$

we get the self-energy in the form

$$\begin{aligned} \Sigma(k, \omega) &= -\frac{\hbar^2}{2m} \int \frac{d^3p}{(2\pi)^3 \rho_0} \mathbf{k} \cdot \left( \frac{\mathbf{k}}{2} + \mathbf{p} \right) Q \left( \left| \frac{\mathbf{k}}{2} + \mathbf{p} \right| \right) \\ &\times \frac{\beta_{\mathbf{k}, \omega}(\mathbf{p})}{\hbar\omega - \varepsilon \left( \left| \frac{\mathbf{k}}{2} + \mathbf{p} \right| \right) - \varepsilon \left( \left| \frac{\mathbf{k}}{2} - \mathbf{p} \right| \right)}. \end{aligned} \quad (165)$$

The function  $\beta_{\mathbf{k},\omega}(\mathbf{p})$  is to be solved self-consistently from the second continuity equation.

The **second continuity equation** then becomes an integral equation for  $\beta_{\mathbf{k},\omega}(\mathbf{p})$ ,

$$\begin{aligned} \beta_{\mathbf{k},\omega}(\mathbf{p}) &= [\hbar\omega - \varepsilon(k)] M_{\mathbf{k}}(\mathbf{p}) + N_{\mathbf{k}}(\mathbf{p}) \\ &+ \int \frac{d^3q}{(2\pi)^3\rho} \frac{\beta_{\mathbf{k},\omega}(\mathbf{q}) [K_{\mathbf{k}}(\mathbf{p}, \mathbf{q}) - \hbar\omega s(|\mathbf{p} - \mathbf{q}|)]}{\hbar\omega - \varepsilon(|\frac{\mathbf{k}}{2} + \mathbf{q}|) - \varepsilon(|\frac{\mathbf{k}}{2} - \mathbf{q}|)}. \end{aligned} \quad (166)$$

With the aid of notations

$$s(\mathbf{k}) = S(\mathbf{k}) - 1 \quad (167)$$

$$s^D(\mathbf{k}) = \delta(\mathbf{k}) + s(\mathbf{k}) \quad (168)$$

we can write the terms appearing in Eq. (166) in the form

$$M_{\mathbf{k}}(\mathbf{p}) = \frac{1}{S(k)} \int \frac{d^3q}{(2\pi)^3\rho} s(|\frac{\mathbf{k}}{2} + \mathbf{q}|) s(|\frac{\mathbf{k}}{2} - \mathbf{q}|) s^D(|\mathbf{p} - \mathbf{q}|) \quad (169)$$

$$\begin{aligned} N_{\mathbf{k}}(\mathbf{p}) &= -\frac{\varepsilon(k)}{k^2} \mathbf{k} \cdot (\frac{\mathbf{k}}{2} + \mathbf{p}) s(|\frac{\mathbf{k}}{2} + \mathbf{p}|) \\ &- \frac{\hbar^2}{2m} \int \frac{d^3q}{(2\pi)^3\rho} (\frac{\mathbf{k}}{2} + \mathbf{p}) \cdot (\frac{\mathbf{k}}{2} + \mathbf{q}) \\ &\quad Q(|\frac{\mathbf{k}}{2} + \mathbf{q}|) s(|\frac{\mathbf{k}}{2} - \mathbf{q}|) s^D(|\mathbf{p} - \mathbf{q}|) \\ &+ (\mathbf{p} \leftrightarrow -\mathbf{p}) \end{aligned} \quad (170)$$

and the kernel is

$$\begin{aligned} K_{\mathbf{k}}(\mathbf{p}, \mathbf{q}) &= \frac{\hbar^2}{2m} \left[ (\frac{\mathbf{k}}{2} + \mathbf{p}) \cdot (\frac{\mathbf{k}}{2} + \mathbf{q}) \right. \\ &\quad \left. [1 - Q(|\frac{\mathbf{k}}{2} + \mathbf{q}|)] s(|\mathbf{p} - \mathbf{q}|) \right. \\ &- \mathbf{k} \cdot (\frac{\mathbf{k}}{2} + \mathbf{q}) Q(|\frac{\mathbf{k}}{2} + \mathbf{q}|) N_{\mathbf{k}}(\mathbf{p}) \\ &- \int \frac{d^3q'}{(2\pi)^3\rho} \left[ (\frac{\mathbf{k}}{2} + \mathbf{p}) \cdot (\mathbf{q} - \mathbf{q}') Q(|\mathbf{q} - \mathbf{q}'|) s(|\frac{\mathbf{k}}{2} - \mathbf{q}'|) \right. \\ &\quad \left. \left. - (\frac{\mathbf{k}}{2} + \mathbf{p}) \cdot (\frac{\mathbf{k}}{2} + \mathbf{q}') Q(|\frac{\mathbf{k}}{2} + \mathbf{q}'|) s(|\mathbf{q} - \mathbf{q}'|) \right] \right] \\ &+ (\mathbf{p} \leftrightarrow -\mathbf{p}). \end{aligned}$$

The collective reference spectrum entering the energy denominator in Eq.(166) is not the Feynman spectrum (1), but the spectrum of Eq. (161), which generally lies closer to the experimental spectrum. Therefore, this approach accounts better for the energetics of the excitations, especially at large momenta.

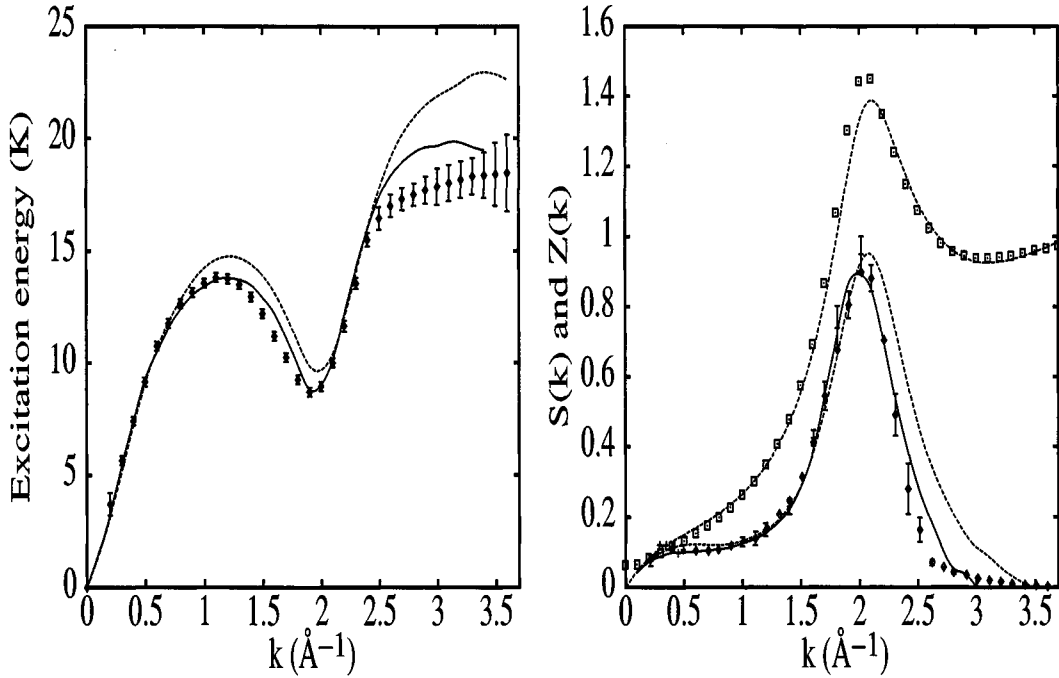


Figure 8: Left figure compares the phonon-roton spectrum of the present theory obtained using the experimental (solid line) and the calculated  $S(k)$  (dashed line) with measurements[40]. In the right figure the experimental[41] (squares) and calculated (dashed line) structure functions are shown together with the pole strength  $Z(k)$  as obtained from the experimental (solid line) and calculated (dashed line)  $S(k)$  and from the measurements.[40]

The continuity equations are solved in momentum space. The center-of-mass momentum  $k$  is a good quantum number and in the space of the relative momentum the continuity equations form an eigenvalue problem. The dependence on the angle between the relative and center-of-mass momenta is taken into account by expanding all the quantities in terms of the Legendre polynomials,

$$\tilde{\Delta}(\mathbf{k}, \mathbf{p}) = \sum_L \tilde{\delta}_L(k, p) P_L(\cos \theta_{\mathbf{k}, \mathbf{p}}) . \quad (171)$$

The resulting eigenvalues are the excitation energies and the eigenvectors give the Fourier transforms of  $\xi(\mathbf{r}_1; t)$  and  $\Delta(\mathbf{r}_1, \mathbf{r}_2; t)$  from which we can calculate the transition currents.



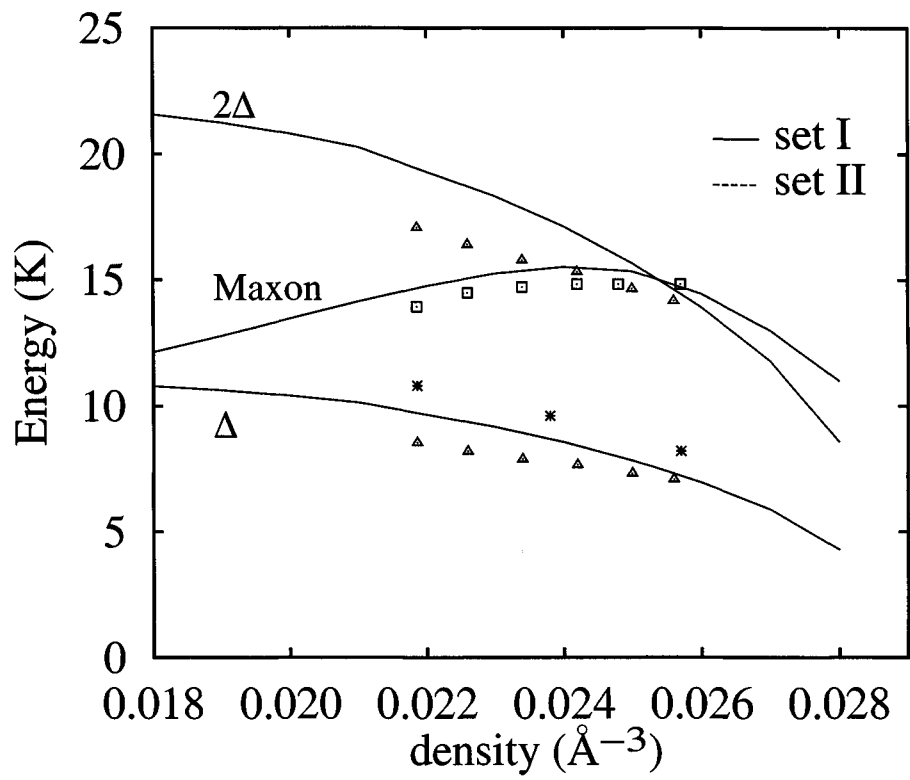


Figure 9: The density dependence of the roton and maxon excitation energies.

### 6.3 Phonon-roton spectrum

The squares are the measured maxon energies and the triangles represent the one- and two-roton energies of Ref. [42]. The stars represent the Brillouin-Wigner perturbation theory results of Chang and Campbell [10]. The solid lines correspond our results. The theoretical maxon energy crosses the two-roton energy between  $0.024$  and  $0.025 \text{ \AA}^{-3}$ , and at higher density the theoretical maxon curve drops with the two-roton curve.

### 6.4 Results on two-particle currents

The two-particle current (149) can be written in the form

$$\mathbf{j}_2(\mathbf{r}_1, \mathbf{r}_2; t) = \rho_0 g_2(|\mathbf{r}_1 - \mathbf{r}_2|) \left\{ \mathbf{j}_1(\mathbf{r}_1; t) + \frac{\hbar \rho_0}{2mi} \tilde{\mathbf{T}}(\mathbf{r}_1, \mathbf{r}_2; t) \right\}, \quad (172)$$

where  $\tilde{\mathbf{T}}(\mathbf{r}_1, \mathbf{r}_2; t)$  depends on the fluctuations in the radial distribution function only,

$$\begin{aligned} \mathbf{T}(\mathbf{r}_1, \mathbf{r}_2; t) &= \nabla_1 \Delta(\mathbf{r}_1, \mathbf{r}_2; t) \\ &- \rho_0 \int d\mathbf{r}_3 \Delta(\mathbf{r}_2, \mathbf{r}_3; t) \mathbf{V}(\mathbf{r}_1, \mathbf{r}_3) \\ &- \rho_0 \int d\mathbf{r}_3 h(\mathbf{r}_2, \mathbf{r}_3) \mathbf{V}(\mathbf{r}_1, \mathbf{r}_3) \\ &\times \left( \xi(\mathbf{r}_3; t) + \Delta(\mathbf{r}_1, \mathbf{r}_3; t) + \Delta(\mathbf{r}_2, \mathbf{r}_3; t) \right). \end{aligned} \quad (173)$$

We have chosen to present our results for the real part of the two-particle current of Eq. (172) in mixed representation as a function of center of mass momentum and relative coordinate. It can then be written in the form

$$\begin{aligned} \mathbf{j}_2(\mathbf{k}, \mathbf{r}, \omega) &= \rho_0 g_2(r) \left[ \mathbf{j}_1(\mathbf{k}, \omega) \cos\left(\frac{1}{2} \mathbf{k} \cdot \mathbf{r}\right) \right. \\ &\left. + \frac{\hbar \rho_0}{2mi} \tilde{\mathbf{T}}(\mathbf{k}, \mathbf{r}, \omega) \right]. \end{aligned} \quad (174)$$

The radial distribution function of the ground state  $g_2(r)$  gives the probability of finding another particle at the distance  $r$  away from a given particle. We locate particle one into the origin and because of the repulsive core of the interaction other particles are repelled outside the radius of about  $2 \text{ \AA}$ . This ‘‘correlation hole’’ is clearly seen in Figs. 10 and 11. We also separate out the oscillating behavior of the sound-like wave where particles move towards each other and away from each other with the wavelength determined by the center-of-mass motion in the cosine term. The more complicated flow patterns are collected into  $\tilde{\mathbf{T}}(\mathbf{k}, \mathbf{r}, \omega)$ . The coordinate system is such that the center of mass momentum points to the z-direction.

Figure 10: The  $z$ -component of the two-particle current (a) at the maxon region  $k = 1.0 \text{ \AA}^{-1}$ , (b) near the roton minimum  $k = 2.0 \text{ \AA}^{-1}$ , (c) at  $k = 2.5 \text{ \AA}^{-1}$ , and (d) in the asymptotic region  $k = 3.0 \text{ \AA}^{-1}$ . The direction of  $\mathbf{k}$  is along the  $x$  axis. (Originally from Ref. [43].)

Figure 11: The short-range part of the two-particle current (a) at the maxon region  $k = 1.0 \text{ \AA}^{-1}$ , (b) near the roton minimum  $k = 2.0 \text{ \AA}^{-1}$ , (c) at  $k = 2.5 \text{ \AA}^{-1}$ , and (d) in the asymptotic region  $k = 3.0 \text{ \AA}^{-1}$ . The direction of  $\mathbf{k}$  is upwards and the tick-mark spacing is  $1.0 \text{ \AA}$ . (Originally from Ref. [43].)

In Fig. 10 we have plotted the  $z$ -component of the two-particle current in four typical cases of the center of mass motion with the wave numbers  $k = 1.0 \text{ \AA}^{-1}$  (maxon),  $2.0 \text{ \AA}^{-1}$  (roton),  $2.5 \text{ \AA}^{-1}$  and  $3.0 \text{ \AA}^{-1}$  (the asymptotic region). Besides the center of mass oscillations there are oscillations due to interparticle correlations. The most pronounced in Fig. 10 is the nearest neighbor peak. From Fig. 10.a one can see that in the maxon region these two kinds of oscillations are out of phase whereas in the roton region of Fig. 10.b they are in phase. That is why the roton region is energetically favored and the minimum corresponds to the wave number of the peak of the structure function  $S(k)$ . This is already well known from the Feynman spectrum  $\hbar^2 k^2 / 2mS(k)$ . When the wavelength becomes shorter than the size of the correlation hole the simple wave pattern breaks down (see Figs. 10.c and 10.d).

A more detailed structure of the current flow is shown in Fig. 11 where we have subtracted the center of mass oscillations. The current flows to the direction of arrows and since it has cylindrical symmetry we show only the  $x - z$ -plane with  $x \geq 0$ . In the maxon and roton regions (Figs. 11.a and 11.b) the dominant feature is the oscillation of the radial distribution function, though some interesting topological structures could be identified. The pattern, however, changes completely at  $2.5 \text{ \AA}^{-1}$ . A clear back flow loop is formed around each atom in Fig. 11.c. The radius of the circulation is of the order of atomic radius (compare with the white area in the figures). When  $k > 2.5 \text{ \AA}^{-1}$  the loop gets elongated with increasing wave number and forms a tube-like structure with a diameter of atomic size. A typical case at  $3.0 \text{ \AA}^{-1}$  is shown in Fig. 11.d.

As a summary we can say that the microscopic, variational method gives good agreement with experiments on the collective excitations obtained as a function of density giving confidence to the equation-of-motion method.

At the roton minimum the size of the correlation hole created by an atom matches with the wave-length of the center-of-mass motion. No backflow motion is seen, but the topological structure of the current requires further investigation. In our wave function we have not put in quantized vortices [23] and the structures seen in Figs. 11.c and 11.d come out of the full optimization of the action integral with respect to the fluctuating one- and two-particle correlation functions. They do not carry any conserved vorticity quantum number. The relation

between these excitations and the vortex excitations should be investigated further.

## 6.5 Precursor of the liquid-solid transition

The liquid-solid phase-transition is a first order transition. Latent heat is required for the liquid to solidify. At the same time there is an abrupt change in the density when the particles in the liquid arrange themselves into the crystal order. Some signatures of the emerging phase transition can be seen in the liquid phase by studying two-particle structures, which break the translational invariance of the liquid phase. We find that by studying solutions of the second Euler equation which break the translational invariance.

We can assume that the single particle density is constant and the system has no center of mass motion. Then the two-particle continuity equation (152) can be written as

$$\begin{aligned} & \frac{\hbar^2}{2m} \nabla_1 \left\{ g_2(\mathbf{r}_1, \mathbf{r}_2) \left[ \nabla_1 \Delta(\mathbf{r}_1, \mathbf{r}_2) - \right. \right. \\ & \left. \left. \rho_0 \int d^3 r_3 g_2(\mathbf{r}_2, \mathbf{r}_3) \mathbf{V}(\mathbf{r}_1, \mathbf{r}_3) \left[ \Delta(\mathbf{r}_1, \mathbf{r}_3) + \Delta(\mathbf{r}_2, \mathbf{r}_3) \right] \right] \right\} \\ & + (1 \leftrightarrow 2) = \hbar \omega g_2(\mathbf{r}_1, \mathbf{r}_2) \Delta(\mathbf{r}_1, \mathbf{r}_2) \end{aligned} \quad (175)$$

Again this equation is simpler to solve in momentum space and since the center of mass momentum  $k = 0$  then  $\tilde{\Delta}(\mathbf{p})$  depends only on the relative momentum  $\mathbf{p}$ , but that is a vector quantity. A convenient way of solving Eq. (175) is to expand  $\Delta(\mathbf{p})$  in terms of Legendre polynomials.

$$\tilde{\Delta}(\mathbf{p}) = \sum_L \tilde{\Delta}_L(p) P_L(\cos \theta_{\mathbf{p}}). \quad (176)$$

The equations for different  $L$ -values separate and those equations can be solved for eigenvalues  $\omega_L$ .

## 6.6 Results in liquid $^4\text{He}$

In  $^4\text{He}$  the first mode to become soft in the long-wavelength limit has in the 3D case the quantum number  $L = 6$  and in the 2D case  $m = 6$  thus indicating the cubic and hexagonal point-group symmetries. The critical densities are  $0.0295 \text{ \AA}^{-3}$  in 3D and  $0.073 \text{ \AA}^{-2}$  in 2D in agreement with the experimental and Monte Carlo results[44, 45, 46] results.

The excitation energies as a function of density are shown in Figs. 12 and 14 and from that we determine the **critical densities**  $0.0295 \text{ \AA}^{-3}$  in the 3D case

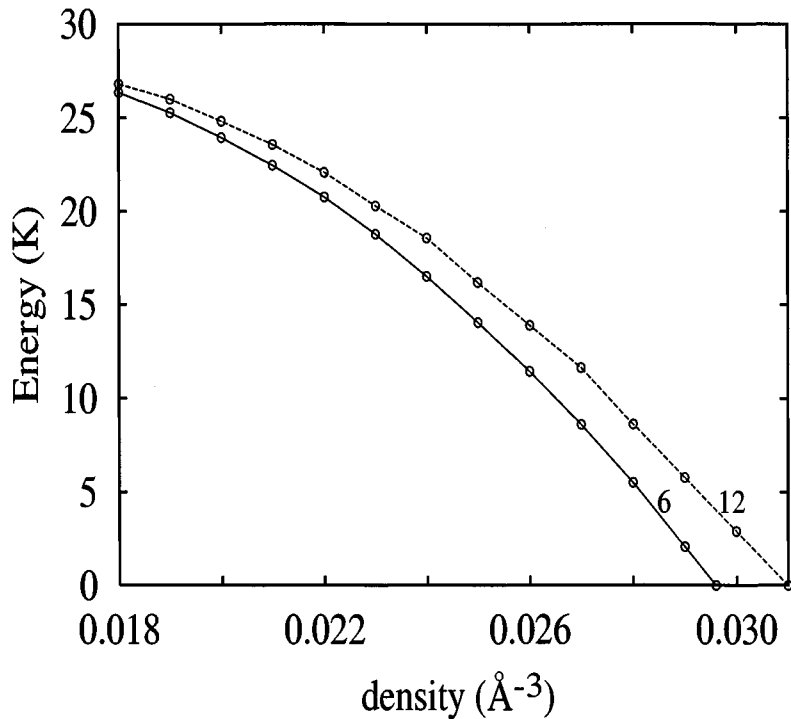


Figure 12: The energies of the  $L = 6$  and  $L = 12$  modes are shown in 3D  ${}^4\text{He}$  at densities 0.022, 0.024 and 0.029  $\text{\AA}^{-3}$ .

and  $0.07\text{\AA}^{-2}$  in 2D at which the energy becomes negative. In the phase diagram those densities are in the phase coexistence region above the solidification density of the liquid but below the melting density of the solid. Our results are in reasonable agreement with experiments in 3D and in 2D with Monte Carlo simulations. In Fig. 13 we also show the eigenfunctions  $\Delta_6(p)$ . The position of the peak determines the **reciprocal lattice vector**  $2.1 \text{\AA}^{-1}$  in 3D and  $1.8 \text{\AA}^{-1}$  in 2D. The width of the peak is related to quantum fluctuations. By studying the Yukawa Bose gas we found out that they decrease with increasing range of the interaction.

## 6.7 Results in charged Yukawa Bose gas

An appealing feature of the Yukawa Bose fluid with the following interaction between particles,

$$V(r) = e^2 \frac{e^{-\mu r}}{r}, \quad (177)$$

is that we can control the range  $1/\mu$  of the interaction and examine the effects on the crystal structure. Our results, shown in Fig. 16, reveal new features in the phase diagrams of these systems. The infinity-range limit gives the  $1/r$ -potential results.

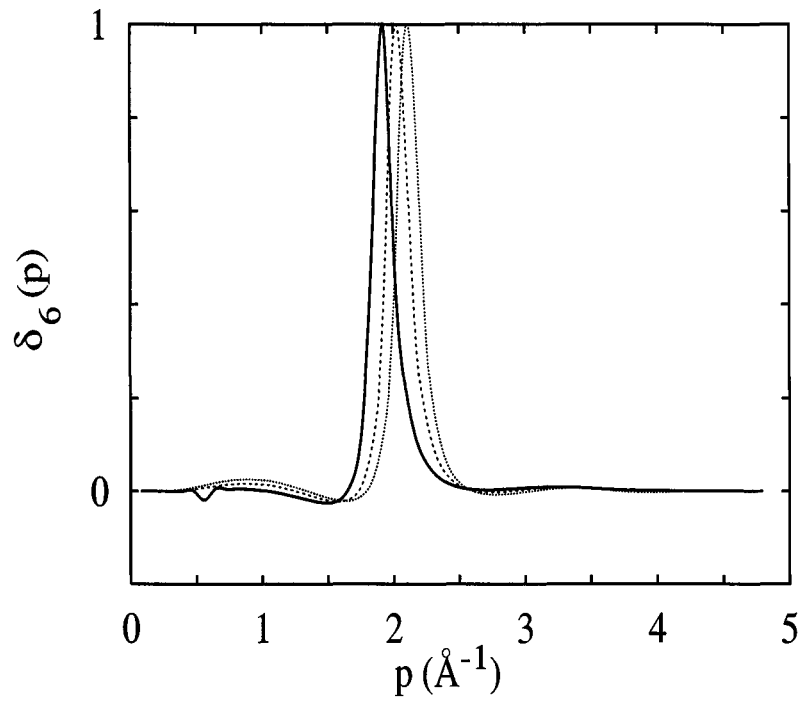


Figure 13: The  $L = 6$  eigenstates are shown in 3D  $^4\text{He}$  at densities 0.022, 0.024 and 0.029  $\text{\AA}^{-3}$ . The peaks of the curves move to the right with increasing density. The vertical scale of the eigenstates is arbitrary.

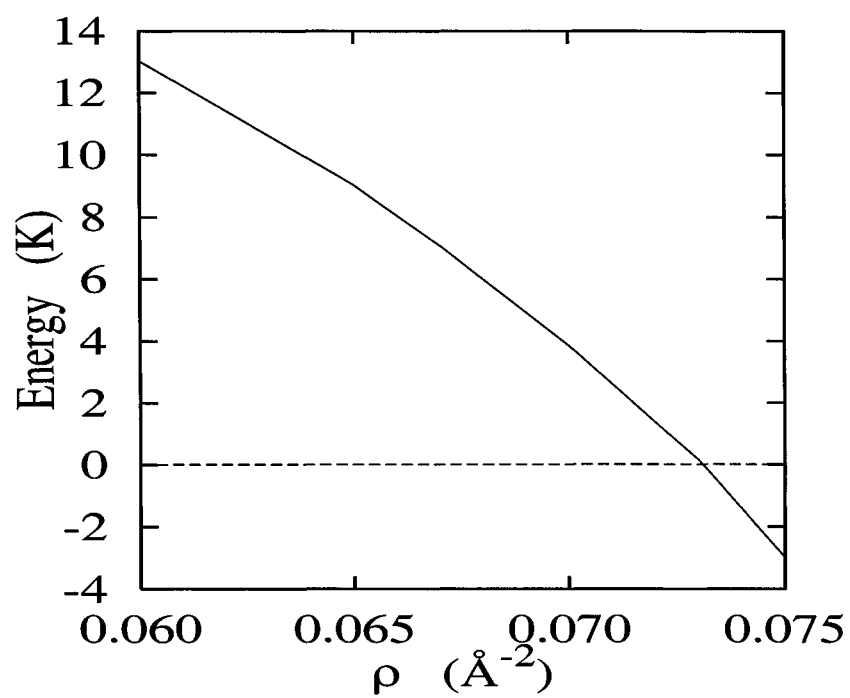


Figure 14: The energies of the  $m = 6$  mode are shown in 2D  ${}^4\text{He}$  at densities 0.060, 0.065, 0.070 and 0.075  $\text{\AA}^{-2}$ .

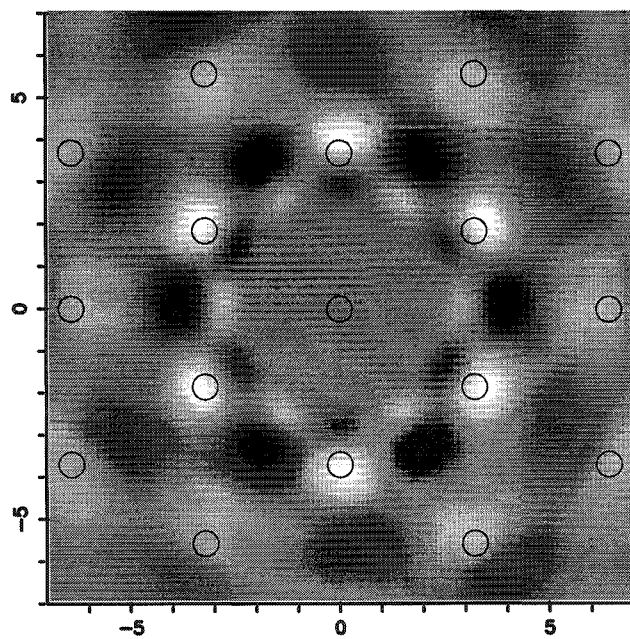


Figure 15: The change in the relative two-body structure corresponding to the first mode to become soft at  $0.070$ . Lighter shade indicates increased probability to find a particle at given coordinates. The gray scale in the middle is the correlation hole. Superimposed rings are the lattice sites in the hexagonal crystal at the same density.



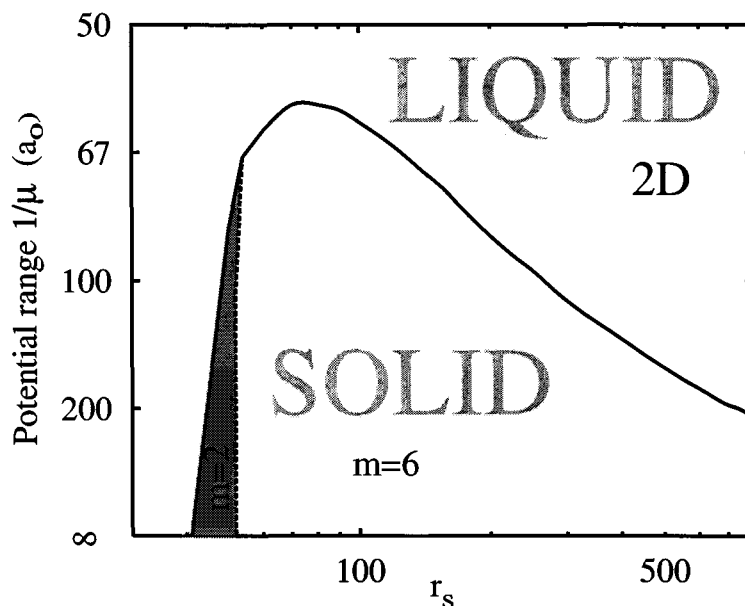


Figure 16: Phase diagrams of the 2D Yukawa Bose fluid as a function of  $r_s$  and the interaction range. The thick solid line separates the liquid and solid phases as obtained from our calculations. In the shaded area the point-group of the most stable structure has the  $m = 2$  symmetry.

The critical values of  $r_s$  for **Wigner crystallization** in the charged Bose fluid are  $r_s = 97$  in 3D and  $r_s = 41$  in 2D, but somewhat unexpectedly the symmetries of the soft modes are  $L = 2$  and  $m = 2$  in 3D and 2D, respectively. As we gradually decrease the range of the potential, we see a change in the critical density. The minimum range at which a Wigner crystal is obtained is  $1/\mu = 138a_0$  in 3D and  $1/\mu = 60a_0$  in 2D in units of the Bohr radius  $a_0$ . Also the point-group symmetry of the soft mode changes from  $L = 2$  to  $L = 6$  symmetry in 3D and similarly from  $m = 2$  to  $m = 6$  symmetry in 2D. A more detailed view of the softening of the modes is given in Fig. 17 for 2D fluid the interaction range is  $1/\mu = 100a_0$ . When  $45 < r_s < 270$  in 2D we find a Wigner crystal, but the point-group symmetry of the crystal structure changes as indicated by the symmetry of the lowest mode.

**In concluding**, our microscopic theory of the soft excitation modes in quantum Bose fluids gives clear indications of the liquid-solid phase transition and the calculated melting densities are in good agreement with experiments and Monte Carlo estimates in the case of  $^4\text{He}$ . Our analysis of the charged fluid both with the  $1/r$  and the Yukawa interaction suggests a new phase with  $L = 2$  ( $m = 2$  in 2D) symmetry between the homogeneous fluid and the cubic (hexagonal in

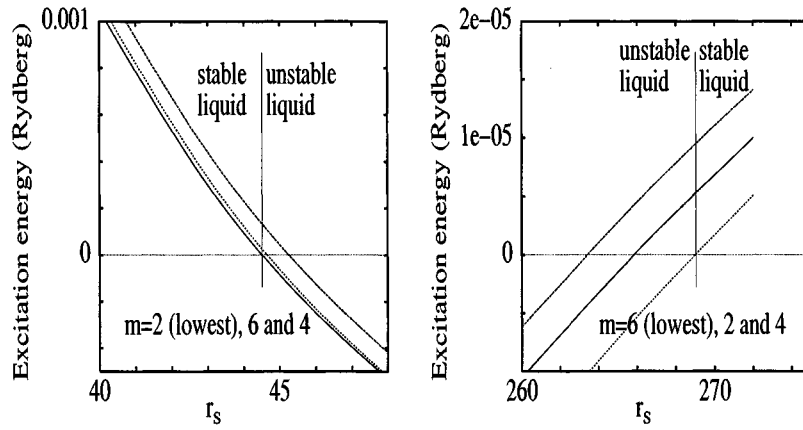


Figure 17: Energies of the lowest excitation modes which become soft in the 2D (upper figure) and 3D (lower figure) Yukawa Bose fluid as a function of  $r_s$ . The range of the interaction  $1/\mu$  is  $100a_0$  in 2D. The quantum numbers of the modes are indicated in the figures.

2D) crystal phases.

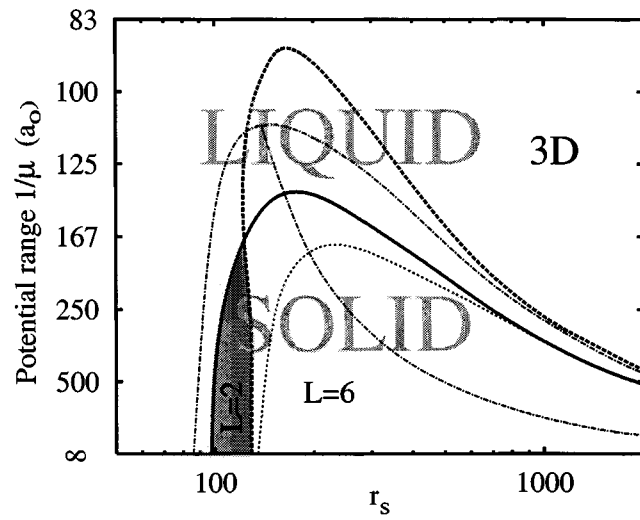


Figure 18: Phase diagrams of the 3D Yukawa Bose fluid as a function of  $r_s$  and the interaction range. The thick solid line separates the liquid and solid phases as obtained from our calculations. The dotted and dashed-dotted lines are the corresponding Green's function and variational Monte Carlo results.[?] The thick dotted line gives the critical density where the  $L = 6$  mode drops below the  $L = 2$  mode. In the shaded area the point-group of the most stable structure has the  $L = 2$  symmetry.

## 7 Sum rules

Sum rules have frequently been applied in estimating various physical properties of quantum liquids, such as ground-state structure and characteristics of the response function, or used as a consistency check for the calculations. We want to see if the proposed theory satisfies known exact sum rules.

We would like to examine specifically the excited states. We therefore consider the  $n$ th energy-moment sum rule, defined as

$$m_n(k) = \int_{-\infty}^{\infty} \frac{d\hbar\omega}{2\pi} (\hbar\omega)^n \Im m\chi(k, \omega). \quad (178)$$

The lowest (raw) moments are

$$S(k) = \int_{-\infty}^{\infty} \frac{d\hbar\omega}{2\pi} S(k, \omega) \quad (179)$$

$$\frac{\hbar^2 k^2}{2m} = \int_{-\infty}^{\infty} \frac{d\hbar\omega}{2\pi} \omega S(k, \omega) d\omega \quad (180)$$

$$\frac{1}{2mc^2} = \lim_{k \rightarrow 0} \int_{-\infty}^{\infty} \frac{d\hbar\omega}{2\pi} \frac{S(k, \omega)}{\omega} d\omega. \quad (181)$$

These sum rules are generally referred to as the zeroth-moment sum rule, the  $f$ -sum rule or the Thomas-Reiche-Kuhn sum rule, and the compressibility sum rule, respectively.

We want to see if these sum rules are satisfied by the linear response function. The notations follow Jackson's notations in Ref. [37],

$$\chi(\mathbf{k}, \omega) = -2S(k)G(\mathbf{k}, \omega) \quad (182)$$

with

$$G(\mathbf{k}, \omega) = \frac{1}{\hbar\omega - \varepsilon(k) + \Sigma(\mathbf{k}, \omega)} \quad (183)$$

In Eq.(113) the self energy was divided into real and imaginary parts

$$\Sigma(k, \omega) = \Delta(\mathbf{k}, \omega) - i\Gamma(\mathbf{k}, \omega) \quad (184)$$

which gives us

$$G(\mathbf{k}, \omega) = \frac{1}{\hbar\omega - \varepsilon(k) - \Delta(\mathbf{k}, \omega) + i\Gamma(\mathbf{k}, \omega)} \quad (185)$$

With these notations the dynamic structure function becomes

$$\begin{aligned} S(\mathbf{k}, \omega) &= -\frac{S(k)}{\pi} \Im m G(\mathbf{k}, \omega) \\ &= \frac{S(k)}{\pi} \frac{\Gamma(\mathbf{k}, \omega)}{[\hbar\omega - \varepsilon(k) - \Delta(\mathbf{k}, \omega)]^2 + \Gamma^2(\mathbf{k}, \omega)} \end{aligned} \quad (186)$$

From the properties of the structure function we know that  $\Gamma(\mathbf{k}, \omega)$  must be a positive function and we can assume that  $\Gamma(\mathbf{k}, \omega) = 0$  when  $\omega < 0$ . We also assume that  $G(\mathbf{k}, \omega)$  is analytic in the upper half plane.

The self energy of our full solution behaves like

$$\lim_{\omega \rightarrow \infty} \Sigma(\mathbf{k}, \omega) = A(k) \quad (187)$$

where  $A(k)$  is a function independent of  $\omega$ .

The  $m_0$  **sum rule** can be easily calculated by choosing the integration path in the upper half plane. Then

$$\begin{aligned} m_0 &= -\frac{S(k)}{\pi} \Im m \int_0^\infty \frac{d(\hbar\omega)}{\hbar\omega - \varepsilon(k) - \Delta(\mathbf{k}, \omega) + i\Gamma(\mathbf{k}, \omega)} \\ &= \frac{S(k)}{\pi} \Im m \lim_{R \rightarrow \infty} \int_0^\pi \frac{iRe^{i\theta} d\theta}{Re^{i\theta} - \varepsilon(k) - \Delta(\mathbf{k}, \omega) + i\Gamma(\mathbf{k}, \omega)} \end{aligned}$$

Giving

$$m_0 = \frac{S(k)}{\pi} \Im m i \int_0^\pi \theta = S(k) \quad (188)$$

In the calculation of the  $m_{-1}$  **sum rule**

$$m_{-1} = -\frac{1}{\pi} \lim_{k \rightarrow 0} S(k) \Im m \int_0^\infty \frac{d(\hbar\omega)}{\hbar\omega} G(\mathbf{k}, \omega) \quad (189)$$

We need to know the limits

$$\begin{aligned} \lim_{R \rightarrow \infty} G(\mathbf{k}, Re^{i\theta}) &= 0 \\ \lim_{r \rightarrow 0} G(\mathbf{k}, re^{i\theta}) &= -\frac{1}{\varepsilon(k) - \Sigma(\mathbf{k}, 0)} \end{aligned} \quad (190)$$

Then

$$\begin{aligned} m_{-1} &= \frac{1}{\pi} \lim_{k \rightarrow 0} S(k) \Im m \int_0^\pi \frac{i\theta}{\varepsilon(k) - \Sigma(\mathbf{k}, 0)} \\ &= \lim_{k \rightarrow 0} \frac{S(k)}{\varepsilon(k) - \Sigma(\mathbf{k}, 0)} \end{aligned} \quad (191)$$

When  $k \rightarrow 0$  then

$$\Sigma(\mathbf{k}, 0) \rightarrow k^2 \quad (192)$$

and we get

$$m_{-1} = \lim_{k \rightarrow 0} \frac{S(k)}{\varepsilon(k)} = \lim_{k \rightarrow 0} \frac{2mS(k)}{\hbar^2 k^2} = \frac{1}{2mc^2} \quad (193)$$

The **f-sum rule** gives some problems if the self-energy does not vanish when  $\omega \rightarrow \infty$

$$\begin{aligned} m_1 &= -\frac{S(k)}{\pi} \Im m \int_0^\infty d(\hbar\omega) \hbar\omega G(\mathbf{k}, \omega) \\ &= \frac{S(k)}{2\pi} \int_0^\infty d(\hbar\omega) \hbar\omega [G(\mathbf{k}, \omega) - G^*(\mathbf{k}, \omega)] \end{aligned} \quad (194)$$

Performing the contour integration as before we get

$$\begin{aligned} m_1 &= \frac{S(k)}{2} [\varepsilon(k) + A(k) + \varepsilon(k) + A^*(k)] \\ &= S(k) [\varepsilon(k) + \Re A(k)] \end{aligned} \quad (195)$$

That does not satisfy the f-sum rule unless the

$$\varepsilon(k) + \Re A(k) = \varepsilon_F(k) = \frac{\hbar^2 k^2}{2mS(k)} \quad (196)$$

In order to show that this is the case we solve the continuity equations in the limit  $\omega \rightarrow \infty$

$$\begin{aligned} \hbar\omega\xi_1(\mathbf{r}_1; t) &= 2U_{\text{ext}}(\mathbf{r}_1; t) + 2\rho_0 \int d^3r_2 h(\mathbf{r}_1, \mathbf{r}_2) U_{\text{ext}}(\mathbf{r}_2; t) \\ \hbar\omega\delta\rho_2(\mathbf{r}_1, \mathbf{r}_2; t) &= 2\rho_0^2 g_2(\mathbf{r}_1, \mathbf{r}_2) [U_{\text{ext}}(\mathbf{r}_1; t) + U_{\text{ext}}(\mathbf{r}_2; t)] \\ &+ 2\rho_0^3 \int d^3r_3 [g_3(\mathbf{r}_1, \mathbf{r}_2, \mathbf{r}_3) - g_2(\mathbf{r}_1, \mathbf{r}_2)] U_{\text{ext}}(\mathbf{r}_3; t) \end{aligned} \quad (197)$$

From the first equation we get  $U_{\text{ext}}(\mathbf{r}_1; t)$

$$\frac{2U_{\text{ext}}(\mathbf{r}_1; t)}{\hbar\omega} = \xi_1(\mathbf{r}_1; t) - \rho_0 \int d^3r_2 X(\mathbf{r}_1, \mathbf{r}_2) \xi(\mathbf{r}_2; t) \quad (198)$$

and insert that into the second equation

$$\begin{aligned} \delta\rho_2(\mathbf{r}_1, \mathbf{r}_2; t) &= \rho^2 g_2(\mathbf{r}_1, \mathbf{r}_2) [\xi(\mathbf{r}_1; t) + \xi(\mathbf{r}_2; t)] \\ &- \rho_0 \int d^3r_3 \xi(\mathbf{r}_3; t) [X(\mathbf{r}_1, \mathbf{r}_3) + X(\mathbf{r}_2, \mathbf{r}_3)] \\ &+ 2\rho_0^3 \int d^3r_3 [g_3(\mathbf{r}_1, \mathbf{r}_2, \mathbf{r}_3) - g_2(\mathbf{r}_1, \mathbf{r}_2)] \\ &\times \left[ \xi(\mathbf{r}_3; t) - \rho \int d^3r_4 X(\mathbf{r}_3, \mathbf{r}_4) \xi(\mathbf{r}_4; t) \right] \end{aligned} \quad (199)$$

We have solved now  $\delta\rho_2(\mathbf{r}_1, \mathbf{r}_2; t)$  entirely in terms of the one-particle density and can insert that back into the one-particle current and show that its divergence gives the Feynman spectrum

$$\mathbf{j}_1(\mathbf{r}_1; t) = \frac{\hbar}{2mi} [\nabla_1 \delta\rho_1(\mathbf{r}_1; t)] \quad (200)$$

$$- \int d^3r_2 \delta\rho_2(\mathbf{r}_1, \mathbf{r}_2; t) \nabla u_2(\mathbf{r}_1, \mathbf{r}_2) \quad (201)$$

$$= \frac{\hbar}{2mi} [\nabla_1 \delta\rho_1(\mathbf{r}_1; t)] \quad (202)$$

$$- \rho_0^2 \int d^3r_2 g_2(\mathbf{r}_1, \mathbf{r}_2) \nabla u_2(\mathbf{r}_1, \mathbf{r}_2) \left[ \xi(\mathbf{r}_1; t) + \xi(\mathbf{r}_2; t) \right]$$

$$\begin{aligned}
& - \rho_0 \int d^3 r_3 \xi(\mathbf{r}_3; t) [X(\mathbf{r}_1, \mathbf{r}_3) + X(\mathbf{r}_2, \mathbf{r}_3)] \\
& - \rho_0^3 \int d^3 r_2 d^3 r_3 [g_3(\mathbf{r}_1, \mathbf{r}_2, \mathbf{r}_3) - g_2(\mathbf{r}_1, \mathbf{r}_2)] \nabla_1 u_2(\mathbf{r}_1, \mathbf{r}_2) \\
& \left[ \xi(\mathbf{r}_3; t) - \rho_0 \int d^3 r_4 X(\mathbf{r}_3, \mathbf{r}_4) \xi(\mathbf{r}_4; t) \right]
\end{aligned} \tag{203}$$

Using the BGY-equations Eqs. (146) and (147) we end up with

$$\begin{aligned}
\mathbf{j}_1(\mathbf{r}_1; t) &= \frac{\hbar}{2mi} \left\{ \nabla_1 \delta \rho_1(\mathbf{r}_1; t) - \rho_0^2 \int d^3 r_2 \nabla_1 g_2(\mathbf{r}_1, \mathbf{r}_2) \right. \\
& \times \left. \left[ \xi(\mathbf{r}_2; t) - \rho_0 \int d^3 r_3 X(\mathbf{r}_2, \mathbf{r}_3) \xi(\mathbf{r}_3; t) \right] \right\}
\end{aligned} \tag{204}$$

Finally using the Ornstein-Zernike relation (23) we get

$$\mathbf{j}_1(\mathbf{r}_1; t) = \frac{\hbar \rho_0}{2mi} \nabla_1 \left[ \xi(\mathbf{r}_1; t) - \rho_0 \int d^3 r_2 \xi(\mathbf{r}_2; t) X(\mathbf{r}_1, \mathbf{r}_2) \right] \tag{205}$$

In the momentum space this gives exactly the Feynman spectrum

$$\mathcal{F} [i\hbar \nabla_1 \cdot \mathbf{j}_1(\mathbf{r}_1; t)] = \frac{\hbar^2 \rho_0}{2m} \frac{k^2}{S(k)} = \rho_0 \varepsilon_F(k) \tag{206}$$

Hence we have shown that the corrections term in collective mode (161) cancels exactly the asymptotic behavior  $A(k)$  in the self energy.

## 8 Dynamics of a single impurity

This section reviews the method[47, 48] to calculate the dynamics of an impurity atom in liquid  $^4\text{He}$  in its ground state. The basic guidelines are the same as for the bulk fluid where we examined pure liquid  $^4\text{He}$ . Therefore, we summarize the necessary generalizations to the basic formalism.

### 8.1 Continuity equations

The start by assuming that the wave function for the ground state of a single impurity atom is optimized. As for the one-component liquid, the dynamics of this system is determined by the response to a weak, external time-dependent perturbation  $U_{\text{ext}}(\mathbf{r}_0; t)$ . The kinematic and dynamic correlations are again separated by writing the wave function in the form

$$\Phi(t) = \frac{e^{-iE_{N+1}t/\hbar}}{\sqrt{\langle \Psi^{(3)}(t) | \Psi^{(3)}(t) \rangle}} \Psi^{(3)}(\mathbf{r}_0, \mathbf{r}_1, \dots, \mathbf{r}_N; t) \quad (207)$$

Here  $E_{N+1}$  is the variational ground-state energy of the system containing the  $N + 1$  particles, and  $\Psi^{(3)}(\mathbf{r}_0, \mathbf{r}_1, \dots, \mathbf{r}_N; t)$  contains the time-dependent correlations,

$$\Psi^{(3)}(\mathbf{r}_0, \mathbf{r}_1, \dots, \mathbf{r}_N; t) = e^{\frac{1}{2}\delta U(\mathbf{r}_1 \dots \mathbf{r}_N)} \Psi^{(3)}(\mathbf{r}_0, \mathbf{r}_1, \dots, \mathbf{r}_N), \quad (208)$$

with

$$\delta U(\mathbf{r}_1 \dots \mathbf{r}_N) = \left[ \delta u^{(3)}(\mathbf{r}_0; t) + \sum_i \delta u^{(34)}(\mathbf{r}_0, \mathbf{r}_i; t) \right] \quad (209)$$

The correlation functions are determined from the action principle

$$\delta S = \delta \int_{t_0}^t dt' \Phi^*(t') \left( H^{(3)} + U_{\text{ext}}(\mathbf{r}_0; t) - i\hbar \frac{\partial}{\partial t'} \right) \Phi(t') = 0, \quad (210)$$

The Hamiltonian of the impurity-background system,  $H^{(3)}$ , is

$$H^{(3)} = H_0 - \frac{\hbar^2}{2m_3} \nabla_0^2 + \sum_{j=1}^N V^{(34)}(|\mathbf{r}_0 - \mathbf{r}_j|). \quad (211)$$

where  $H_0$  is obtained from Eq. (2) for  $N_3 = 1$ .

The variation with respect to  $\delta u^{(3)}(\mathbf{r}_0; t)$  and  $\delta u^{(34)}(\mathbf{r}_0, \mathbf{r}_i; t)$  leads to the continuity equations

$$\nabla_0 \cdot \mathbf{j}^{(3)}(\mathbf{r}_0; t) + \frac{\partial}{\partial t} \delta \rho^{(3)}(\mathbf{r}_0; t) = \frac{2\rho^{(3)}}{\hbar} U_{\text{ext}}(\mathbf{r}_0; t) \quad (212)$$

and

$$\begin{aligned} \nabla_0 \cdot \mathbf{j}^{(34)}(\mathbf{r}_0, \mathbf{r}_1; t) + \nabla_1 \cdot \mathbf{J}^{(34)}(\mathbf{r}_0, \mathbf{r}_1; t) \\ + \frac{\partial}{\partial t} \delta \rho^{(34)}(\mathbf{r}_0, \mathbf{r}_1; t) = \frac{2}{\hbar} U_{\text{ext}}(\mathbf{r}_0; t) \rho^{(34)}(\mathbf{r}_0, \mathbf{r}_1). \end{aligned} \quad (213)$$



The transition currents are defined in terms of the fluctuating one-particle density and pair correlation function,

$$\mathbf{j}^{(3)}(\mathbf{r}_0; t) = \frac{\hbar}{2m_3 i} \left[ \nabla_0 \delta \rho^{(3)}(\mathbf{r}_0; t) \right. \quad (214)$$

$$\left. - \int d^3 r_1 \delta u^{(34)}(\mathbf{r}_0, \mathbf{r}_1; t) \nabla_0 \rho^{(34)}(\mathbf{r}_0, \mathbf{r}_1) \right],$$

$$\mathbf{j}^{(34)}(\mathbf{r}_0, \mathbf{r}_1; t) = \frac{1}{\rho^{(3)}} \mathbf{j}^{(3)}(\mathbf{r}_0; t) \rho^{(34)}(\mathbf{r}_0, \mathbf{r}_1) \quad (215)$$

$$+ \frac{\hbar}{2m_3 i} \left[ \rho^{(34)}(\mathbf{r}_0, \mathbf{r}_1) \nabla_0 \delta u^{(34)}(\mathbf{r}_0, \mathbf{r}_1; t) \right.$$

$$+ \int d^3 r_2 \left[ \rho^{(344)}(\mathbf{r}_0, \mathbf{r}_1, \mathbf{r}_2) - \frac{1}{\rho^{(3)}} \rho^{(34)}(\mathbf{r}_0, \mathbf{r}_1) \rho^{(34)}(\mathbf{r}_0, \mathbf{r}_2) \right]$$

$$\left. \nabla_2 \delta u^{(34)}(\mathbf{r}_0, \mathbf{r}_2; t) \right],$$

and

$$\mathbf{J}^{(34)}(\mathbf{r}_0, \mathbf{r}_1; t) = \frac{\hbar}{2m_4 i} \rho^{(34)}(\mathbf{r}_0, \mathbf{r}_1) \nabla_1 \delta u^{(34)}(\mathbf{r}_0, \mathbf{r}_1; t). \quad (216)$$

The ground-state quantities needed here are the impurity-background pair and triplet distribution functions  $\rho^{(34)}(\mathbf{r}_0, \mathbf{r}_1)$  and  $\rho^{(344)}(\mathbf{r}_0, \mathbf{r}_1, \mathbf{r}_2)$ , respectively.

## 8.2 Linear response and self energy

The poles of the linear response function

$$\chi^{(3)}(k, \omega) = \frac{\delta \rho^{(3)}(k, \omega)}{\rho^{(3)} \tilde{U}_{\text{ext}}(k, \omega)} \quad (217)$$

determine the elementary excitation modes, which are obtained by setting  $\tilde{U}_{\text{ext}}(k, \omega) = 0$ . This leads to the implicit equation

$$\hbar \omega = \frac{\hbar^2 k^2}{2m_3} + \Sigma^{(3)}(k, \omega) \quad (218)$$

with the self-energy

$$\Sigma^{(3)}(k, \omega) = \frac{\hbar^2}{2m_3} \int \frac{d^3 p}{(2\pi)^3 \rho^{(4)}} \frac{\mathbf{k} \cdot \mathbf{p} S^{(34)}(p) \beta_{\mathbf{k}, \omega}^{(34)}(\mathbf{p})}{[\hbar \omega - t^{(3)}(\mathbf{k} + \mathbf{p}) - \varepsilon^{(4)}(p)]}. \quad (219)$$

Here  $S^{(34)}(p)$  is the  ${}^3\text{He}$ - ${}^4\text{He}$  structure function,  $t^{(3)}(k)$  the kinetic energy of the impurity, and  $\varepsilon^{(4)}(p)$  the background phonon-roton spectrum. The function  $\beta_{\mathbf{k}, \omega}^{(34)}(\mathbf{p})$  is to be solved from the second continuity equation (214).

The result is

$$\beta_{\mathbf{k},\omega}^{(34)}(\mathbf{p}) = \hbar\omega \frac{\mathbf{k} \cdot \mathbf{p}}{k^2} \frac{S^{(34)}(p)}{S^{(44)}(p)} \quad (220)$$

$$- \int \frac{d^3q}{(2\pi)^3 \rho^{(4)}} \frac{\beta_{\mathbf{k},\omega}^{(34)}(\mathbf{q}) K_{\mathbf{k},\omega}(\mathbf{p}, \mathbf{q})}{[\hbar\omega - t^{(3)}(\mathbf{k} + \mathbf{q}) - \varepsilon^{(4)}(q)]}$$

with the kernel

$$K_{\mathbf{k},\omega}(\mathbf{p}, \mathbf{q}) = S^{(44)}(q)$$

$$\left\{ \left[ \left( S^{(34)}(|\mathbf{p} - \mathbf{q}|) + 1 \right) \tilde{u}^{(344)}(\mathbf{p} - \mathbf{q}, -\mathbf{p}, \mathbf{q}) \right. \right.$$

$$\left. \left. + S^{(34)}(|\mathbf{p} - \mathbf{q}|) \left[ \hbar\omega - \frac{(\mathbf{k} + \mathbf{p}) \cdot (\mathbf{k} + \mathbf{q})}{p^2} t^{(3)}(p) \right] \right\}$$

$$- S^{(34)}(|\mathbf{p} - \mathbf{q}|) \frac{\mathbf{p} \cdot \mathbf{q}}{p^2} \varepsilon^{(4)}(p). \quad (221)$$

The linear response function has then a simple form

$$\chi^{(3)}(k, \omega) = \frac{2}{\hbar\omega - t^{(3)}(k) - \Sigma^{(3)}(k, \omega)} \quad (222)$$

Again, note that the self energy can become complex in case the denominator in Eq. (219) is positive for some value of  $\mathbf{p}$ ,

$$\max_{\mathbf{p}} \left[ \hbar\omega - t^{(3)}(\mathbf{k} + \mathbf{p}) - \varepsilon^{(4)}(p) \right] > 0. \quad (223)$$

If this condition is satisfied, then it is kinematically possible that the  $^3\text{He}$  impurity loses energy by emitting a phonon-roton mode  $\varepsilon^{(4)}(p)$  while making a transition into a low-energy impurity mode  $t^{(3)}(\mathbf{k} + \mathbf{p})$ .

The strength of the pole  $Z(k)$  can be evaluated from the derivative of the self energy,

$$Z(k) = \left[ 1 - \frac{d\Sigma^{(3)}(k, \omega)}{d(\hbar\omega)} \Big|_{\omega=\omega_p} \right]^{-1}. \quad (224)$$

Note also that the singularity structure of Eq. (220) is the same as that of the self energy. For real frequencies  $\omega$  the imaginary part of  $\beta_{\mathbf{k},\omega}^{(34)}(\mathbf{q})$  is zero if the energy denominator is negative for all values of  $\mathbf{q}$ . Modes with an energy  $\hbar\omega$  high enough to satisfy the inequality (223) can decay into a phonon-roton mode and the solution has a non-zero imaginary part.

### 8.3 Hydrodynamic effective mass

The long-wavelength limit of the excitation energy defines the hydrodynamic effective mass  $m_H^*$ ,

$$\hbar\omega = \frac{\hbar^2 k^2}{2m_H^*}, \quad \text{when } k \rightarrow 0. \quad (225)$$

Inserting this into Eq. (218) we get

$$\frac{m_H^*}{m_3} = \frac{1}{1 - I} \quad (226)$$

with

$$I = \lim_{k \rightarrow 0^+} \frac{1}{k^2} \int \frac{d^3 p}{(2\pi)^3 \rho^{(4)}} \frac{\mathbf{k} \cdot \mathbf{p} S^{(34)}(p) \beta_{\mathbf{k}, \omega_0}^{(34)}(\mathbf{p})}{t^{(3)}(p) + \varepsilon^{(4)}(p)}, \quad (227)$$

where  $\omega_0 = \hbar k^2 / 2m_H^*$ . Using Eqs. (224) and (225), we find that in the long-wavelength limit the pole strength is inversely proportional to the effective mass,

$$\lim_{k \rightarrow 0} Z(k) = \frac{m_3}{m_H^*}. \quad (228)$$

In the so-called “uniform limit approximation”[6] one neglects all *coordinate-space* products of two functions, *i.e.* we approximate, for example,  $\rho^{(34)}(\mathbf{r}_0, \mathbf{r}_1) \delta u^{(34)}(\mathbf{r}_0, \mathbf{r}_1) \approx \rho^{(3)} \rho^{(4)} \delta u^{(34)}(\mathbf{r}_0, \mathbf{r}_1)$ , but *convolution products* are retained. Then,  $\beta_{\mathbf{k}, \omega_0}^{(34)}(\mathbf{p})$  has a simple form[47]

$$\beta_{\mathbf{k}, \omega_0}^{(34)}(\mathbf{p}) = \frac{\hbar^2}{2m_3} \mathbf{k} \cdot \mathbf{p} \frac{S^{(34)}(p)}{S^{(44)}(p)}. \quad (229)$$

This, together with the equations (226) and (227), gives the “un-renormalized effective mass” derived by Owen.[49]

### 8.4 Results

Table 1: Pressure dependence of the hydrodynamic effective mass from various calculations and experiments. The second column contains the result of our microscopic calculation, the next two column contains the hydrodynamic effective mass as obtained from the fit to the experiments of Refs. [50] and [51].

$P$ (atm)	$m_H^*/m$		
	This work	Ref. [50]	Ref. [51]
0	2.09	2.18	2.15
5	2.22	2.31	
10	2.34	2.44	2.39
15	2.45	2.54	
20	2.55	2.64	2.62

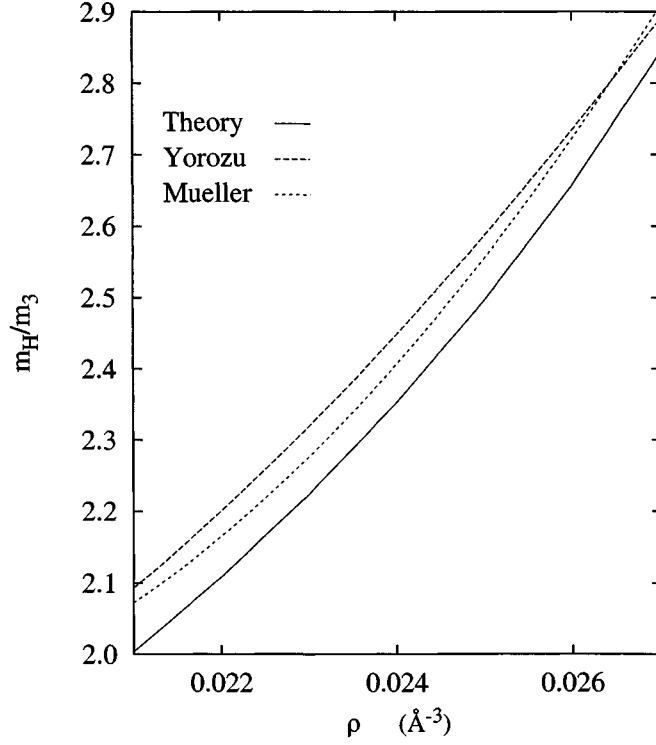


Figure 19: Our theoretical hydrodynamic mass (solid line), and our zero-concentration extrapolations of the data of Ref. [50] (long dashed line) and [51] (short dashed line).

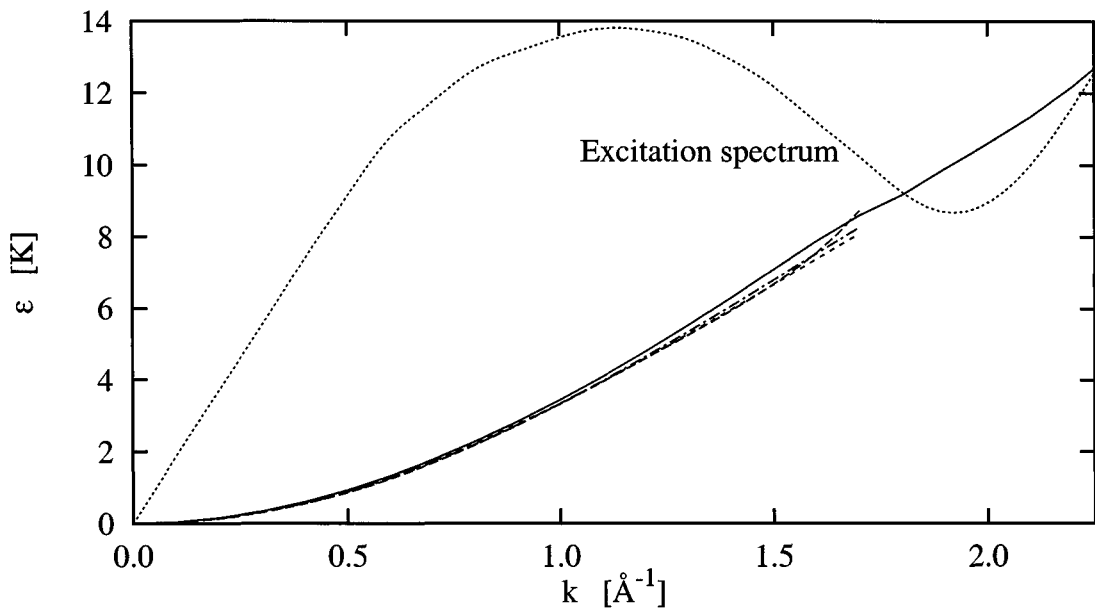


Figure 20: The excitation spectrum of the  $^3\text{He}$  impurity. The solid curve is the result of the present theory. It is compared with the measurements by Greywall (Ref. [52]) (long dashed line), Fåk *et al.* (Ref. [53]) (short dashed line) and Owers-Bradley *et al.* (Ref. [54]) (dash-dotted line). The dotted line shows, for reference, the experimental phonon-roton spectrum.[40]

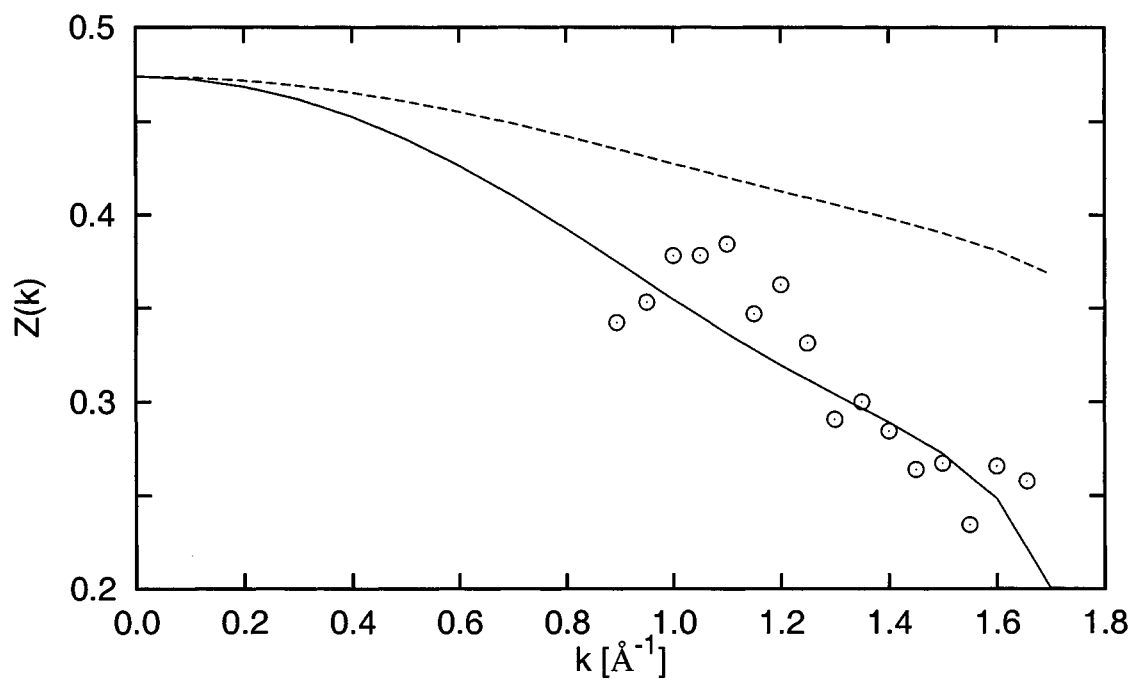


Figure 21: The pole strength of the elementary impurity excitation mode is plotted as a function of momentum (solid line). The measured strength of the particle-hole excitation at 1% concentration and saturation vapor pressure from Fig. 11 of Ref. [53] is shown with circles. For comparison we also show the effective mass as a function of momentum.

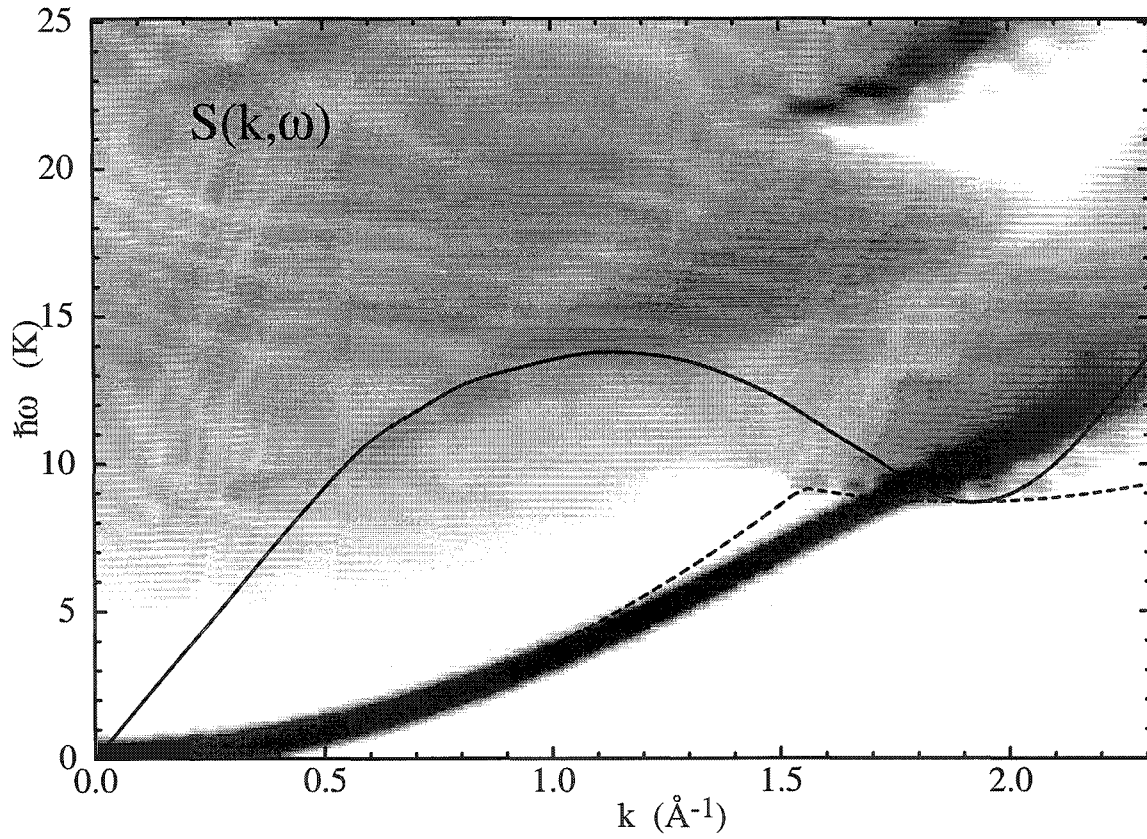


Figure 22: The impurity dynamic structure function  $S^{(3)}(k, \omega)$  plotted in the  $k, \omega$  plane. Also shown are the phonon-roton spectrum of the background  ${}^4\text{He}$  (heavy solid line, the data are from [40]), and the decay threshold of the impurity excitation mode (dashed line).

## 9 Summary

Detailed derivation of the equation of motion method has been described to you. It is a general method which can be applied to study dynamic of quantum Bose systems. I have pointed out its strengths and weaknesses for applications ranging from single impurity dynamics to liquid-solid phase transition. Many aspect of the method require more work and clever new ideas.



## References

- [1] H. Glyde, *Excitations in liquid and solid helium* (Oxford University Press, Oxford, 1994).
- [2] L. Landau, J. Phys. U.S.S.R. **5**, 71 (1941).
- [3] N. N. Bogoliubov, J. Phys. U.S.S.R. **9**, 23 (1947).
- [4] R. P. Feynman, Phys. Rev. **94**, 262 (1954).
- [5] R. P. Feynman and M. Cohen, Phys. Rev. **102**, 1189 (1956).
- [6] E. Feenberg, *Theory of Quantum Fluids* (Academic, New York, 1969).
- [7] J. W. Clark, in *Progress in Particle and Nuclear Physics*, edited by D. H. Wilkinson (Pergamon Press Ltd., Oxford, 1979), Vol. 2, pp. 89–199.
- [8] H. W. Jackson and E. Feenberg, Ann. Phys. (NY) **15**, 266 (1961).
- [9] H. W. Jackson and E. Feenberg, Rev. Mod. Phys. **34**, 686 (1962).
- [10] C. C. Chang and C. E. Campbell, Phys. Rev. B **13**, 3779 (1976).
- [11] S. Manousakis and V. R. Pandharipande, Phys. Rev. B **30**, 5062 (1984).
- [12] L. Reatto, S. A. Vitiello, and G. L. Masserini, J. Low Temp. Phys. **93**, 879 (1993).
- [13] S. Moroni, L. Reatto, and S. Fantoni, Czech. J. Phys. Suppl. S1 **46**, 281 (1996).
- [14] G. A. Williams, Phys. Rev. Lett. **68**, 2054 (1992).
- [15] C. H. Aldrich and D. Pines, J. Low Temp. Phys. **25**, 677 (1976).
- [16] H. R. Glyde and A. Griffin, Phys. Rev. Lett. **65**, 1454 (1990).
- [17] A. Griffin, *Excitations in a Bose-Condensed Liquid* (Cambridge University Press, Cambridge, 1993), pp. 1–308.
- [18] V. L. Berezinskii, Sov. Phys. JETP **32**, 493 (1971).
- [19] J. M. Kosterlitz and D. J. Thouless, J. Phys. C **6**, 1181 (1973).
- [20] R. J. Donnelly, *Quantized Vortices in Helium II* (Cambridge University Press, Cambridge, 1991).
- [21] M. Saarela, B. E. Clements, E. Krotscheck, and F. V. Kusmartsev, J. Low Temp. Phys. **93**, 971 (1993).
- [22] M. Saarela and F. V. Kusmartsev, Physica B **194-196**, 617 (1994).
- [23] Saarela and F. V. Kusmartsev, Phys. Lett. A **202**, 317 (1995).

- [24] M. Saarela, Phys. Rev. B **33**, 4596 (1986).
- [25] M. Saarela and J. Suominen, in *Condensed Matter Theories*, edited by J. S. Arponen, R. F. Bishop, and M. Manninen (Plenum, New York, 1988), Vol. 3, pp. 157–165.
- [26] J. Suominen and M. Saarela, in *Condensed Matter Theories*, edited by J. Keller (Plenum, New York, 1989), Vol. 4, p. 377.
- [27] E. Krotscheck, Phys. Rev. B **31**, 4258 (1985).
- [28] C. E. Campbell, in *Progress in Liquid Physics*, edited by C. A. Croxton (Wiley, London, 1977), Chap. 6, pp. 213–308.
- [29] B. E. Clements *et al.*, Phys. Rev. B **50**, 6958 (1994).
- [30] V. Apaja *et al.*, Phys. Rev. B **55**, 12925 (1997).
- [31] A. K. Kerman and S. E. Koonin, Ann. Phys. (NY) **100**, 332 (1976).
- [32] P. Kramer and M. Saraceno, *Geometry of the time-dependent variational principle in quantum mechanics*, Vol. 140 of *Lecture Notes in Physics* (Springer, Berlin, Heidelberg, and New York, 1981).
- [33] B. E. Clements, E. Krotscheck, and C. J. Tymczak, Phys. Rev. B **53**, 12253 (1996).
- [34] C. E. Campbell, Phys. Lett. A **44**, 471 (1973).
- [35] C. C. Chang and C. E. Campbell, Phys. Rev. B **15**, 4238 (1977).
- [36] E. Krotscheck, Phys. Rev. B **33**, 3158 (1986).
- [37] H. W. Jackson, Phys. Rev. A **9**, 964 (1974).
- [38] F. Dalfovo and S. Stringari, Phys. Rev. B **46**, 13991 (1992).
- [39] J. Mathews and R. L. Walker, *Mathematical Methods of Physics*, 2nd ed. (Benjamin, New York, 1970), p. 131.
- [40] R. A. Cowley and A. D. B. Woods, Can. J. Phys. **49**, 177 (1971).
- [41] H. N. Robkoff and R. B. Hallock, Phys. Rev. B **24**, 159 (1981).
- [42] O. W. Dietrich, E. H. Graf, C. H. Huang, and L. Passell, Phys. Rev. A **5**, 1377 (1972).
- [43] V. Apaja and M. Saarela, Phys. Rev. B **57**, 5358 (1998).
- [44] S. Giorgini, J. Boronat, and J. Casulleras, Phys. Rev. B **54**, 6099 (1996).
- [45] P. A. Whitlock, G. V. Chester, and M. H. Kalos, Phys. Rev. B **38**, 2418 (1988).

- [46] M. C. Gordillo and D. M. Ceperley, *Phys. Rev. B* **58**, 6447 (1998).
- [47] M. Saarela and E. Krotscheck, *J. Low Temp. Phys.* **90**, 415 (1993).
- [48] M. Saarela, in *Recent Progress in Many Body Theories*, edited by Y. Avishai (Plenum, New York, 1990), Vol. 2, pp. 337–346.
- [49] J. C. Owen, *Phys. Rev. B* **23**, 5815 (1981).
- [50] S. Yorozu, H. Fukuyama, and H. Ishimoto, *Phys. Rev. B* **48**, 9660 (1993).
- [51] R. Simons and R. M. Mueller, *Czechoslovak Journal of Physics Suppl.* **46**, 201 (1996).
- [52] D. S. Greywall, *Phys. Rev. B* **20**, 2643 (1979).
- [53] B. Fåk *et al.*, *Phys. Rev. B* **41**, 8732 (1990).
- [54] J. R. Owers-Bradley *et al.*, *J. Low Temp. Phys.* **72**, 201 (1988).